

Variability and stability of anthropogenic CO₂ in Antarctic Bottom Water observed in the Indian sector of the Southern Ocean, 1978-2018

Léo Mahieu¹, Claire Lo Monaco², Nicolas MetzI², Jonathan Fin², Claude Mignon²

¹Ocean Sciences, School of Environmental Sciences, University of Liverpool, 4 Brownlow Street, Liverpool L69 3GP, UK

²LOCEAN-IPSL, Sorbonne Université, CNRS/IRD/MNHN Paris, France

Correspondence to: Léo Mahieu (Leo.Mahieu@Liverpool.ac.uk); Claire Lo Monaco (claire.lomonaco@locean.upmc.fr)

Abstract

Antarctic bottom water (AABW) is known as a long term sink for anthropogenic CO₂ (C_{ant}) but the sink is hardly quantified because of the scarcity of the observations, specifically at an interannual scale. We present in this manuscript an original dataset combining 40 years of carbonate system observations in the Indian sector of the Southern Ocean (Enderby Basin) to evaluate and interpret the interannual variability of C_{ant} in the AABW. This investigation is based on regular observations collected at the same location (63° E-56.5° S) in the framework of the French observatory OISO from 1998 to 2018 extended by GEOSECS and INDIGO observations (1978, 1985 and 1987).

At this location the main sources of AABW sampled is the low-saline Cape Darnley Bottom Water (CDBW) and the Weddell Sea Deep Water (WSDW). Our calculations reveal that C_{ant} concentrations increased significantly in the AABW, from the average concentration of 7 μmol.kg⁻¹ calculated for the period 1978-1987 to the average concentration of 13 μmol.kg⁻¹ for the period 2010-2018. This is comparable to previous estimates in other Southern Ocean (SO) basins, with the exception of bottom waters close to their formation sites where C_{ant} concentrations are about twice as large. Our analysis shows that total carbon (C_T) and C_{ant} increasing rates in the AABW are about the same over the period 1978-2018, and we conclude that the long-term change in C_T is mainly due to the uptake of C_{ant} in the different formation regions. This is, however, modulated by significant interannual to multi-annual variability associated with variations in hydrographic (potential temperature (Θ), salinity (S)) and biogeochemical (C_T, total alkalinity (A_T), dissolved oxygen (O₂)) properties. A surprising result is the apparent stability of C_{ant} concentrations in recent years despite the increase in C_T and the gradual acceleration of atmospheric CO₂. The interannual variability at play in AABW needs to be carefully considered on the extrapolated estimation of C_{ant} sequestration based on sparse observations over several years.

1 Introduction

Carbon dioxide (CO₂) atmospheric concentration has been increasing since the start of the industrialization (Keeling and Whorf, 2000). This increase leads to an ocean uptake of about a quarter of C_{ant} emissions (Le Quééré et al., 2018; Gruber et al., 2019a). It is widely acknowledged that the Southern Ocean (SO) is responsible for 40 % of the C_{ant} ocean sequestration (Matear, 2001; Orr et al., 2001; McNeil et al., 2003; Gruber et al., 2009;

37 Khatiwala et al., 2009). Ocean C_{ant} uptake and sequestration have the benefit to limit the atmospheric CO_2 increase
38 but also result in a gradual decrease of the ocean pH (Gattuso and Hansson, 2011; Jiang et al., 2019). Understanding
39 the oceanic C_{ant} sequestration and its variability is of major importance to predict future atmospheric CO_2
40 concentrations, impact on the climate and impact of the pH change on marine ecosystems (de Baar, 1992; Orr et
41 al., 2005; Ridgwell and Zeebe, 2005).

42 C_{ant} in seawater cannot be measured directly and the evaluation of the relatively small C_{ant} signal from the total
43 inorganic dissolved carbon (C_T ; less than 3 %; Pardo et al, 2014) is still a challenge to overcome. Different
44 approaches have been developed in the last 40 years to quantify C_{ant} concentrations in the oceans. The ‘historical’
45 back calculation method based on C_T measurement and preformed inorganic carbon estimate (C^0) was
46 independently published by Brewer (1978) and Chen and Millero (1979). This method has been often applied at
47 regional and basin scale (Chen, 1982; Poisson and Chen, 1987; Chen, 1992; Goyet et al., 1998; Körtzinger et al.,
48 1998, 1999; Lo Monaco et al., 2005a). More recently the TrOCA method (Tracer combining Oxygen, dissolved
49 Carbon and total Alkalinity) has been developed (Touratier and Goyet, 2004a, b; Touratier et al., 2007) and applied
50 in various regions including the SO (e.g. Lo Monaco et al., 2005b; Sandrini et al., 2007; Van Heuven et al., 2011;
51 Pardo et al., 2014; Shadwick et al., 2014; Roden et al., 2016; Kerr et al., 2018). Comparisons with other data-based
52 methods show significant differences in C_{ant} concentrations, especially at high latitudes and more particularly in
53 deep and bottom waters (Lo Monaco et al., 2005b; Vázquez-Rodríguez et al., 2009; Pardo et al., 2014).

54 Antarctic bottom water (AABW) are of specific interest for the atmospheric CO_2 and heat regulation as they play
55 a major role in the meridional overturning circulation (Johnson et al., 2008; Marshall and Speer, 2012). AABW
56 represent a large volume of water by covering a major part of the world ocean floor (Mantyla and Reid, 1995), and
57 their spreading in the interior ocean through circulation and water mixing is a key mechanism for the long-term
58 sequestration of C_{ant} and climate regulation (Siegenthaler and Sarmiento, 1993). The AABW formation is a specific
59 process occurring in few locations around the Antarctic continent (Orsi et al., 1999). In short, the AABW formation
60 occurs when the Antarctic surface waters flows down along the continental shelf. The Antarctic surface waters
61 density required for this process to happen is reached by the increase in salinity (S) due to brine release from the
62 ice formation and by a decrease in temperature due to heat loss to either the ice-shelf or the atmosphere.
63 Importantly, AABW formation process is enhanced by katabatic winds that open areas free of ice called polynyas
64 (Williams et al., 2007). Indeed, katabatic winds are responsible for an intense cooling that enhance the formation
65 of ice constantly pushed away by the wind, leading to cold and salty surface waters in contact with the atmosphere.
66 The variable conditions of wind, ice production, surface water cooling and continental slope shape encountered
67 around the Antarctic continent lead to different types of AABW, hence the AABW characteristics can be used to
68 identify their formation sites.

69 The ability of AABW to accumulate C_{ant} has been controversial since one can believe that the ice coverage limits
70 the invasion of C_{ant} in Antarctic surface waters (e.g. Poisson and Chen, 1987). This is, however, not the case in
71 polynyas, and several studies have reported significant C_{ant} signals in AABW formation regions, likely due to the
72 uptake of CO_2 induced by high primary production (Sandrini et al., 2007; van Heuven et al., 2011, 2014; Shadwick
73 et al., 2014; Roden et al., 2016). However, little is known about the variability and evolution of the CO_2 fluxes in
74 AABW formation regions, and since biological and physical processes are strongly impacted by seasonal and
75 interannual climatic variations (Fukamachi et al., 2000; Gordon et al., 2010, McKee et al., 2011; Gordon et al.,
76 2015; Gruber et al., 2019b), the amount of C_{ant} stored in the AABW may be very variable, which could bias the

77 estimates of C_{ant} trends derived from data sets collected several years apart (e.g. Williams et al., 2015; Pardo et al.,
78 2017; Murata et al., 2019).

79 In this context of potentially high variability in C_{ant} uptake at AABW formation sites, as well as in AABW export,
80 circulation and mixing, we used repeated observations collected in the Indian sector of the Southern Ocean to
81 explore the variability in C_{ant} and C_T in the AABW and evaluate their evolution over the last 40 years.

82 **2 Study area**

83 **2.1 AABW circulation in the Atlantic and Indian sectors of the Southern Ocean**

84 The circulation in the SO is dominated by the Antarctic Circumpolar Current (ACC) that flows eastward, while
85 the Coastal Antarctic Current (CAC) flows westward (Carter et al., 2008). The ACC and the CAC influence the
86 circulation of the entire water column and generate gyres, crucial drivers of SO circulation (Carter et al., 2008).

87 The most important gyres encountered around the Antarctic continent correspond to major AABW formation sites
88 (Fig. 1). The main AABW formation sites are the Weddell Sea, where Weddell Sea Deep Water and Weddell Sea
89 Bottom Water are produced (WSDW and WSBW, respectively; Gordon, 2001; Gordon et al., 2010), the Ross Sea
90 for the Ross Sea Bottom Water (RSBW; Gordon et al., 2009, 2015), the Adelie Land coast for the Adelie Land
91 Bottom Water (ALBW; Williams et al., 2008, 2010) and the Cape Darnley Polynya for the Cape Darnley Bottom
92 Water (CDBW; Ohshima et al., 2013). AABW formation has also been observed in the Prydz Bay (Yabuki et al.,
93 2006; Rodehacke et al., 2007). There, three polynyas and two ice shelves have been identified as Prydz Bay Bottom
94 Water (PBBW) production hotspots from seal tagging and mooring data (Williams et al., 2016). This PBBW flows
95 out the Prydz Bay through the Prydz Channel and get mixed with the CDBW. The mix of CDBW and PBBW
96 (hereafter called CDBW) represents a significant AABW export (13 % of all AABW exports; Ohshima et al.,
97 2013).

98 The largest bottom water source of the global ocean is the Weddell Sea (Gordon et al., 2001). The exported WSDW
99 is a mixture of the WSBW and Warm Deep Water (WDW). The WDW is a slightly modified Lower Circumpolar
100 Deep Water (LCDW) by mixing with high salinity surface water when the LCDW enters the Weddell basin (see
101 Fig. 2 in van Heuven et al., 2011). The WSDW mixes with the LCDW during its transit. A part of the WSDW
102 deflecting southward with the ACC in the Enderby Basin reaches the north-western part of the Princess Elizabeth
103 Trough (PET) region (area separating the Kerguelen Plateau from the Antarctic continent), where it mixes with
104 other types of AABW (Heywood et al., 1999; Orsi et al., 1999). The deepest point of the PET is 3750 m, deep
105 enough to allow AABW to flow between the Australian Antarctic Basin and the Enderby Basin (Heywood et al.,
106 1999).

107 At the east of the PET, the CAC transports a mixture of RSBW and ALBW and accelerates northward along the
108 eastern side of the Kerguelen Plateau (Mantyla and Reid, 1995; Fukamachi et al., 2010) following the Australian-
109 Antarctic gyre, also called Kerguelen gyre (Vernet et al. 2019). Part of the ALBW-RSBW mixture reaches the
110 western side of the Kerguelen Plateau by the southern part of the PET (Heywood et al., 1999; Orsi et al., 1999;
111 Van Wijk and Rintoul, 2014) and mixes with the CDBW. The mixture of CDBW and ALBW-RSBW flows
112 westward with the CAC and dilutes with the LCDW (Meijers et al., 2010) until it reaches the Weddell gyre (Carter
113 et al., 2008).

114 Figure 1

115 **2.2 AABW definition**

116 The distinction of water masses is usually performed according to neutral density (γ^n) layers. In the SO, LCDW
117 and AABW properties are generally well defined in the range 28.15-28.27 kg.m⁻³ and 28.27-bottom, respectively
118 (Orsi et al., 1999; Murata et al 2019). However, to interpret the long-term variability of the properties in the AABW
119 core at our location, we prefer to adjust the AABW definition to a narrow (more homogeneous) layer that we call
120 Lower Antarctic Bottom Water (LAABW), characterised by $\gamma^n > 28.35$ kg.m⁻³ (roughly ranging from 4200m to
121 4800m, see Fig. 3). This definition corresponds to the AABW characteristics observed at higher latitudes in the
122 Indian SO sector (Roden et al., 2016). The layer above the LAABW is hereafter called Upper Antarctic Bottom
123 Water (UAABW).

124 **3 Material and methods**

125 **3.1 AABW sampling during the last 40 years**

126 Most of the data used in this study were obtained in the framework of the long-term observational project OISO
127 (Ocean Indien Service d'Observations) conducted since 1998 onboard the R.S.V. Marion-Dufresne (IPEV/TAAF).
128 During these cruises, several stations are visited, but only one station is sampled down to the bottom (4800 m)
129 south of the Polar Front, at 63.0° E and 56.5° S (hereafter noted OISO-ST11). This station is located in the Enderby
130 Basin on the Western side of the Kerguelen Plateau (Fig. 1) and coincides with the station 75 of the INDIGO-3
131 cruise (1987). In our analysis, we included all the data available for the OISO-ST11 location (which has not been
132 sampled during each cruise for logistic reasons). We also included data from the station 14 (deepest sample taken
133 at 5109 m) of the INDIGO-1 cruise (1985) and the station 430 (deepest sample taken at 4710 m) of the GEOSECS
134 cruise (1978) located near OISO-ST11 sampling site (405 km and 465 km away from it, respectively; Fig. 1). All
135 the re-occupations used in this analysis are listed in Table 1. Since seasonal variations are only observed in the
136 surface mixed layer (Metzl et al., 2006), we used the observations available for all seasons (Table 1).

137 Table 1

138 **3.2 Validation of the data**

139 For 1998-2004, the OISO data were quality controlled in CARINA (Lo Monaco et al., 2010) and for 2005 and
140 2009-2011 in GLODAPv2 (Key et al., 2015; Olsen et al., 2016, 2019). The 3 additional datasets from GEOSECS,
141 INDIGO-1 and INDIGO-3 were first qualified in GLODAPv1 (Key et al., 2004) and used for the first C_{ant} estimates
142 in the Indian Ocean (Sabine et al., 1999). The adjustments recommended for these historical datasets have been
143 revisited in CARINA and GLODAPv2. In this paper we used the revised adjustments applied to the GLODAPv2
144 data product, with one exception for the total alkalinity (A_T) data from INDIGO-3 for which we applied an
145 intermediate adjustment between the recommendation from GLODAPv1 (confirmed in CARINA) for no
146 adjustment (in reason of the lack of available observations in this region for robust comparison) and the adjustment
147 by $-8 \mu\text{mol.kg}^{-1}$ applied to the GLODAPv2 data product (justification in Supp. Mat.).

148 For the recent OISO cruises conducted in 2012-2018 not yet included in the most recent GLODAPv2 product, we
149 have proceeded to a data quality control in deep waters where C_{ant} concentrations are low and subject to very small
150 changes from year to year (see Supp. Mat.).

151 3.3 Biogeochemical measurements

152 Measurement methods during OISO cruises were previously described (Jabaud-Jan et al., 2004; Metzl et al., 2006).
153 In short, measurements were obtained using Conductivity-Temperature-Depth (CTD) casts fixed on a 24 bottles
154 rosette equipped with 12 L General Oceanics Niskin bottles. Potential temperature (Θ) and salinity (S)
155 measurements have an accuracy of 0.002 °C and 0.005 respectively. A_T and C_T were sampled in 500 mL glass
156 bottles and poisoned with 100 μ L of mercuric chloride saturated solution to halt biological activity. Discrete C_T
157 and A_T samples were analyzed onboard by potentiometric titration derived from the method developed by Edmond
158 (1970) using a closed cell. The repeatability for C_T and A_T varies from 1 to 3.5 $\mu\text{mol.kg}^{-1}$ (depending on the cruise)
159 and is determined by sample duplicates (in surface, at 1000 m and in bottom waters). The accuracy of C_T and A_T
160 measurements (always better than $\pm 3 \mu\text{mol.kg}^{-1}$ for all cruises since 1998) was ensured by daily analyses of
161 Certified Reference Materials (CRMs) provided by A.G. Dickson laboratory (Scripps Institute of Oceanography).
162 Dissolved oxygen (O_2) concentration was determined by an oxygen sensor fixed on the rosette. These values were
163 adjusted using measurements obtained by Winkler titrations using a potentiometric titration system (at least 12
164 measurements for each profile). The thiosulphate solution used for the Winkler titration was calibrated using iodate
165 standard solution (provided by Ocean Scientific International Limited) to ensure the standard O_2 accuracy of 2
166 $\mu\text{mol.kg}^{-1}$. Nitrate (NO_3) and silicate (Si) concentrations were measured onboard or onshore with an automatic
167 colorimetric Technicon analyser following the methods described by Tréguer and Le Corre (1975) until 2008, and
168 the revised protocol described by Coverly et al. (2009) since 2009. Based on replicate measurements for deep
169 samples we estimate an error of about 0.3 % for both nutrients. NO_3 data are not available for all the cruises used
170 in this analysis. The mean NO_3 concentrations in the LAABW at OISO-ST11 is $32.8 \pm 1.2 \mu\text{mol.kg}^{-1}$ while the
171 average value derived from the GLODAP-v2 database in bottom waters south of 50°S in the South Indian Ocean
172 is $32.4 \pm 0.6 \mu\text{mol.kg}^{-1}$. The lack of NO_3 data for few cruises has been palliated by using a climatological value of
173 $32.4 \mu\text{mol.kg}^{-1}$ with a limited impact on C_{ant} determined by the C° method ($< 2 \mu\text{mol.kg}^{-1}$ on estimates based on
174 the differences observed between NO_3 measurements and the climatological value).

175 3.4 C_{ant} calculation using the TrOCA method

176 The TrOCA method was first presented by Touratier and Goyet (2004a, b) and revised by Touratier et al. (2007).
177 Following the concept of the quasi-conservative tracer NO (Broecker, 1974), TrOCA is a tracer defined as a
178 combination of O_2 , C_T and A_T , following:

$$179 \quad \text{TrOCA} = O_2 + a \left(C_T - \frac{1}{2} A_T \right), \quad (1)$$

180 where a is defined in Touratier et al. (2007) as combination of the Redfield equation coefficients for CO_2 , O_2 ,
181 HPO_4^{2-} and H^+ . For more details about the definition and the calibration of this parameter, please refer to Touratier
182 et al. (2007). The temporal change in TrOCA is independent of biological processes and can be attributed to
183 anthropogenic carbon (Touratier and Goyet, 2004a). Therefore, C_{ant} can be directly calculated from the difference
184 between TrOCA and its pre-industrial value TrOCA° :

$$185 \quad C_{\text{ant}} = \frac{\text{TrOCA} - \text{TrOCA}^\circ}{a}, \quad (2)$$

186 where TrOCA° is evaluated as a function of θ and A_T (Eq. 3):

$$187 \quad \text{TrOCA}^\circ = e^{\left[b - (c) \cdot \theta - \frac{d}{A_T^2} \right]}, \quad (3)$$

188 In these expressions, coefficients a, b, c and d were adjusted by Touratier et al. (2007) from deep waters free of
 189 anthropogenic CO₂ using the tracers Δ¹⁴C and CFC-11 from the GLODAPv1 database (Key et al., 2004). The final
 190 expression used to calculate C_{ant} is:

$$191 \quad C_{ant} = \frac{O_2 + 1.279 \left(C_T - \frac{1}{2} A_T \right) - e^{\left[\frac{7.511 - (1.087 \cdot 10^{-2}) \cdot \theta - \frac{7.81 \cdot 10^5}{A_T^2} \right]}}{1.279}, \quad (4)$$

192
 193 The consideration of the errors on the different parameters involved in the TrOCA method results in an uncertainty
 194 of ±6.25 μmol.kg⁻¹ (mostly due to the parameter a, leading to ±3.31 μmol.kg⁻¹). As this error is relatively large
 195 compared to the expected Cant concentrations in deep and bottom SO waters (Pardo et al., 2014) we will compare
 196 the TrOCA results using another indirect method to interpret C_{ant} changes over 40 years.

197 **3.5 C_{ant} calculation using the preformed inorganic carbon (C⁰) method**

198 To support the C_{ant} trend determined with the TrOCA method, C_{ant} was also estimated using a back-calculation
 199 approach noted C⁰ (Brewer, 1978; Chen and Millero, 1979), previously adapted for C_{ant} estimates along the
 200 WOCE-I6 section between South Africa and Antarctica (Lo Monaco et al., 2005a). This method consists in the
 201 correction of the measured C_T for the biological contribution (C_{bio}) and the preindustrial preformed C_T (C⁰_{PI}):

$$202 \quad C_{ant} = C_T - C_{bio} - C_{PI}^0, \quad (5)$$

203 C_{bio} (Eq. 6) depends on carbonate dissolution and organic matter remineralization, taking account of the corrected
 204 C/O₂ ratio from Kortzinger et al. (2001):

$$205 \quad C_{bio} = 0.5 \Delta A_T - (C/O_2 + 0.5 N/O_2) \Delta O_2, \quad (6)$$

206 Where C/O₂ = 106/138 and N/O₂ = 16/138. ΔA_T and ΔO₂ are the difference between the measured values (A_T and
 207 O₂) and the preformed values (A_T⁰ and O₂⁰). A_T⁰ (Eq. 7) has been computed by Lo Monaco et al. (2005a) as a
 208 function of Θ, S and the conservative tracer PO:

$$209 \quad A_T^0 = 0.0685 PO + 59.79 S - 1.45 \theta + 217.1, \quad (7)$$

210 PO (Eq. 8) has been defined by Broecker (1974) and depends on the equilibrium of O₂ with phosphate (PO₄). When
 211 PO₄ data are not available, nitrate (NO₃) can be used instead as follows (the N/P ratio of 16 is from Anderson and
 212 Sarmiento, 1994):

$$213 \quad PO = O_2 + 170 PO_4 = O_2 + (170/16) NO_3, \quad (8)$$

214 To determine O₂⁰, it is assumed that the surface water is in full equilibrium with the atmosphere (O₂⁰ = O_{2,sat}; Benson
 215 and Krause, 1980) and that after subduction O₂ in a given water mass is only impacted by the biological activity
 216 (Weiss, 1970). A correction of O₂⁰ has been proposed by Lo Monaco et al. (2005a) to take account of the
 217 undersaturation of O₂ due to sea-ice cover at high latitudes. O₂⁰ is, therefore, corrected by assuming a mean mixing
 218 ratio of the ice-covered surface waters k=50 % (Lo Monaco et al., 2005a), and a mean value for O₂ undersaturation
 219 in ice-covered surface waters α = 12 % (Anderson et al., 1991) according to Eq. 9:

$$220 \quad \Delta O_2 = (1 - \alpha k) O_{2,sat} - O_2 = AOU, \quad (9)$$

221 C⁰_{PI} in equation 5 is a function of the current preformed C_T (C⁰_{obs}) and a reference water term (Eq. 10):

$$222 \quad C_{PI}^0 = C_{obs}^0 + [C_T - C_{bio} - C_{obs}^0]_{REF}, \quad (10)$$

223 C_{0,obs} has been computed similarly as A_T⁰ (Eq. 11):

$$224 \quad C_{obs}^0 = -0.0439 PO + 42.79 S - 12.02 \theta + 739.8, \quad (11)$$

225 Where the reference water term is a constant for a given time of observation, corresponding to the time when C^0_{obs}
226 is parameterized. In this paper, we used the parameterization given by Lo Monaco et al., (2005a) and their
227 estimated value for the reference term of $51 \mu\text{mol.kg}^{-1}$. This number has been computed using an optimum
228 multiparametric (OMP) model to estimate the mixing ratio of the North Atlantic deep water in the SO (used as
229 reference water, i.e. old water mass where $C_{\text{ant}} = 0$). For more details about the C^0 method, which has a final error
230 of $\pm 6 \mu\text{mol.kg}^{-1}$, please see Lo Monaco et al. (2005a).

231 **4 Results**

232 The vertical distribution of hydrological and biogeochemical properties observed in deep and bottom waters and
233 their evolution over the last 40 years are displayed in Fig 2. The LCDW layer ($\gamma^n = 28.15\text{-}28.27 \text{ kg.m}^{-3}$) is
234 characterized by minimum O_2 concentrations (Fig. 2c), higher C_T (Fig. 2b) and lower C_{ant} concentrations than in
235 the AABW (Fig. 2a). C_{ant} concentrations were not significant in the LCDW until the end of the 1990s ($<6 \mu\text{mol.kg}^{-1}$),
236 then our data show an increase in C_{ant} between the two 1998 reoccupations, followed by relatively constant C_{ant}
237 concentrations ($10 \pm 3 \mu\text{mol.kg}^{-1}$). In the LAABW ($\gamma^n > 28.35 \text{ kg.m}^{-3}$), well identified by low Θ , low S and high O_2 ,
238 C_{ant} concentrations are higher than in the overlying UAABW and LCDW (Fig. 2a). The evolutions of the mean
239 properties in the LAABW over 40 years are shown in Fig. 3. In this layer, C_{ant} concentrations increased from 5 ± 4
240 $\mu\text{mol.kg}^{-1}$ in 1978 and $7 \pm 4 \mu\text{mol.kg}^{-1}$ in the mid-1980s to $13 \pm 2 \mu\text{mol.kg}^{-1}$ at the end of the 1990s and up to 19 ± 2
241 $\mu\text{mol.kg}^{-1}$ in 2004 (Fig. 3a). Figure 3a also shows a very good agreement between the TrOCA method and the C^0
242 method for both the magnitude and variability of C_{ant} in the LAABW. Our results show a mean C_{ant} trend in the
243 LAABW of $+1.4 \mu\text{mol.kg}^{-1}.\text{decade}^{-1}$ over the full period and a maximum trend of the order of $+5.2 \mu\text{mol.kg}^{-1}.$
244 decade^{-1} over 1987-2004 (Table 2). Due to the mixing of AABW with old CDW (C_{ant} free), these trends are lower
245 than the theoretical trend expected from the increase in atmospheric CO_2 . Indeed, assuming that the surface ocean
246 $f\text{CO}_2$ follows the atmospheric growth rate ($+1.8 \mu\text{atm.year}^{-1}$ over 1978-2018) in the seasonal ice zone (Roden et
247 al., 2016), the theoretical C_{ant} trend at the AABW formation sites would be of the order of $+8 \mu\text{mol.kg}^{-1}.\text{decade}^{-1}$
248 in the Antarctic surface water. This is close to the theoretical C_T trend estimated for freezing shelf water in the
249 Weddell Sea (van Heuven et al 2014).

250 Figure 2

251 Over the full period, C_T increased by $2.0 \pm 0.5 \mu\text{mol.kg}^{-1}.\text{decade}^{-1}$, mostly due to the accumulation of C_{ant} (Table
252 2). Our data also show a significant decrease in O_2 concentrations by $0.8 \pm 0.4 \mu\text{mol.kg}^{-1}.\text{decade}^{-1}$ over the 40-years
253 period (Fig. 3c, Table 2) that could be caused by reduced ventilation, as suggested by Schmidtko et al. (2017) who
254 observed significant O_2 loss in the global ocean. In the deep Indian SO sector, these authors found a trend
255 approaching $-1 \mu\text{mol.kg}^{-1}.\text{decade}^{-1}$ over 50 years (1960-2010), which is consistent with our data. We did not detect
256 any significant trend in A_T , Θ and S over the full period, but on shorter periods our data show a significant decrease
257 in A_T . The low A_T values observed over 2000-2004 (Fig. 3d) could suggest reduced calcification in the upper
258 ocean leading to less sinking of calcium carbonate tests and a decrease in A_T in deep and bottom waters over this
259 period (Fig. 2d). For this period the increase in C_T was lower than the accumulation of C_{ant} , but such feature is
260 disputable in view of the uncertainty on the C_{ant} calculation. This event is followed by an increase in the 'natural'
261 component of C_T (C_{nat} , calculated as the difference between C_T and C_{ant}) since 2004 associated to a decrease in O_2
262 and no increase in C_{ant} (Table 2). These trends were not associated with a significant trend in θ or S (Fig. 3e,f,
263 Table 2). The increase in C_{nat} is thus unlikely originating from increased mixing with LCDW during bottom waters

264 transport, confirming that our LAABW definition exclude mixing with the LCDW. Enhanced organic matter
265 remineralization is also unlikely since NO_3 did not show any significant trend (Table 2).

266 Table 2

267 Figure 3

268 Importantly, our data show substantial interannual variations in LAABW properties, which could significantly
269 impact the trends estimated from limited reoccupations (e.g. Williams et al., 2015; Pardo et al., 2017; Murata et
270 al., 2019). For example, we found relatively higher C_{ant} concentrations in 1985 ($10 \mu\text{mol.kg}^{-1}$) compared to 1978
271 ($5 \mu\text{mol.kg}^{-1}$) and 1987 ($7 \mu\text{mol.kg}^{-1}$). This is linked to a signal of low S in 1985 (Fig. 3f) that could be due to a
272 larger contribution of fresher waters such as the WSDW or CDBW. This could also be related to the different
273 sampling locations. Over the last decade (2009-2018), our data show large and rapid changes in S that are partly
274 reflected on C_T and O_2 , and that could explain the relatively low C_{ant} concentrations observed over this period.
275 Indeed, the S maximum observed in 2012 (correlated to higher θ) is associated with a marked C_T minimum
276 (surprisingly almost as low as in 1987), as well as low A_T (hence low $C_{T\text{nat}}$), and low NO_3 concentrations. Since
277 these anomalies were associated with a decrease in C_{ant} concentrations, one may argue for an increased contribution
278 of bottom waters ventilated far away from our study site. A few years later our data show a S minimum (correlated
279 to lower θ), associated with a rapid increase in C_T and a rapid decrease in O_2 between 2013 and 2016, suggesting
280 the contribution of a closer AABW type such as the CDBW. The freshening of $-0.006 \text{ decade}^{-1}$ in S between 2004
281 and 2018 that we observed on the western side of the Kerguelen Plateau was also observed on the eastern side of
282 the Plateau by Menezes et al. (2017) over a similar period. In this region, Menezes et al. (2017) evaluated a change
283 in S by about $-0.008 \text{ decade}^{-1}$ from 2007 to 2016 (against $-0.002 \text{ decade}^{-1}$ between 1994 and 2007), suggesting an
284 acceleration of the AABW freshening in recent years. However, they also reported a warming by $+0.06 \text{ }^\circ\text{C.decade}^{-1}$,
285 while we observed cooler temperature in 2016-2018. This suggests that we sampled a different mixture of
286 AABW.

287 Figure 4

288 5 Discussion

289 5.1 LAABW composition at OISO-ST11

290 At each formation site, AABW experiences significant temporal property changes, mostly recognized at decadal
291 scale (e.g. freshening in the South Indian Ocean, Menezes et al., 2017) with potential impact on carbon uptake and
292 C_{ant} concentrations during AABW formation (Shadwick et al., 2013). The Θ -S diagram constructed from yearly
293 averaged data in bottom waters (Fig. 4) shows that the LAABW at OISO-ST11 is a complex mixture of WSDW,
294 CDBW, RSBW and ALBW. The coldest type of LAABW was observed at the GEOSECS station at 60° S (-0.56
295 $^\circ\text{C}$), while the warmer type of LAABW observed at the INDIGO-1 station at 53° S ($-0.44 \text{ }^\circ\text{C}$). These extreme Θ
296 values could be a natural feature or may be related to specific sampling. For the other cruises, Θ in LAABW ranges
297 from -0.51 to $-0.45 \text{ }^\circ\text{C}$ with no clear indication on the specific AABW origin. The S range observed in the bottom
298 waters at OISO-ST11 (34.65-34.67) illustrates either changes in mixing with various AABW sources or temporal
299 variations at the formation site. Given the knowledge of deep and bottom waters circulation and characteristics
300 (Fig. 1 and 4) and the significant C_{ant} concentrations that we calculated in the LAABW (Fig. 3a), the main
301 contribution at our location is likely the younger and colder CDBW for which relatively high C_{ant} concentrations

302 have been recently documented (Roden et al., 2016). From its formation region, the CDBW can either flow
303 westward with the CAC or flow northward in the Enderby Basin (Ohshima et al., 2013, Fig. 1). In the CAC branch,
304 the CDBW mixes with the LCDW along the Antarctic shelf and the continental slope between 80° E and 30° E
305 (Meijers et al., 2010; Roden et al., 2016). On the western side of the Kerguelen Plateau, CDBW also mixes with
306 RSBW and ALBW (Orsi et al., 1999; Van Wijk and Rintoul, 2014). In this context, the C_{ant} concentrations
307 observed in the bottom layer at OISO-ST11 are probably not linked to one single AABW source, but are likely a
308 complex interplay of AABW from different sources with different biogeochemical properties.

309 **5.2 C_{ant} concentrations**

310 In order to compare our C_{ant} estimates with other studies, we separated the 40-years time-series into 3 periods: the
311 first period (1978-1987) corresponds to historical data when C_{ant} is expected to be low; the second period (1998-
312 2004) starts when the first OISO cruise was conducted (and using CRMs for A_T and C_T measurements) and ends
313 when C_{ant} concentrations in the LAABW are maximum (Fig. 3a); the third period consists in the observations
314 performed in late 2009 to 2018 when the observed variations are relatively large for S and small for C_{ant} . The mean
315 C_{ant} concentrations for each period are 7, 14 and 13 $\mu\text{mol.kg}^{-1}$, respectively, which is consistent with the results
316 from other studies (Table 3). The C_{ant} values for 1978-1987 can hardly be compared to other studies because very
317 few observations were conducted in the 1980s in the Indian sector of the SO (Sabine et al., 1999) and because of
318 potential biases for historical data despite their careful quality control in GLODAP and CARINA (Key et al., 2004;
319 Lo Monaco et al., 2010; Olsen et al., 2016). In addition, the different methods used to estimate C_{ant} can lead to
320 different results, especially in deep and bottom waters of the SO (Vázquez-Rodríguez et al., 2009). Overall, Table
321 3 confirms that C_{ant} concentrations were low in the 1970s and 1980s, and reached values of the order of 10 $\mu\text{mol.kg}^{-1}$
322 in the 1990s, a signal not clearly captured in global data-based estimates (Gruber, 1998; Sabine et al., 2004;
323 Waugh et al., 2006; Khatiwala et al., 2013).

324 The observations presented in this analysis, although regional, offer a complement to recent estimates of C_{ant}
325 changes evaluated between 1994 and 2007 in the top 3000 m for the global ocean (Gruber et al., 2019a). In the
326 Enderby Basin at the horizon 2000-3000 m, the accumulation of C_{ant} from 1994 to 2007 is not uniform and ranges
327 between 0 and 8 $\mu\text{mol.kg}^{-1}$ (Gruber et al., 2019a). At our station, in the LCDW (2000-3000 m) the C_{ant}
328 concentrations were not significant in 1978-1987 (-2 to 5 $\mu\text{mol.kg}^{-1}$) but increase to an average of 9 ± 3 $\mu\text{mol.kg}^{-1}$
329 in 1998-2018 (Fig. 2a), probably due to mixing with AABW that contain more C_{ant} . Interestingly, this value is
330 close but in the high range of the C_{ant} accumulation estimated from 1994 to 2007 in deep waters of the south Indian
331 Ocean (Gruber et al., 2019a).

332 Not surprisingly, high C_{ant} concentrations are detected in the AABW formation regions (Table 3). The highest C_{ant}
333 concentrations in bottom waters (up to 30 $\mu\text{mol.kg}^{-1}$) were observed in the ventilated shelf waters in the Ross Sea
334 (Sandrini et al., 2007). In the Adélie and Mertz Polynya regions, Shadwick et al. (2014) observed high C_{ant}
335 concentrations in the subsurface shelf waters (40-44 $\mu\text{mol.kg}^{-1}$) but lower values in the ALBW (15 $\mu\text{mol.kg}^{-1}$) due
336 to mixing with older LCDW. In WSBW, all C_{ant} concentrations estimated from observations between 1996 and
337 2005 and with the TrOCA method (Table 3) lead to about the same values ranging between 13 and 16 $\mu\text{mol.kg}^{-1}$
338 (Lo Monaco et al., 2005b; van Heuven et al., 2011). In bottom waters formed near the Cape Darnley (CDBW),
339 Roden et al. (2016) estimated high C_{ant} concentrations in bottom waters (25 $\mu\text{mol.kg}^{-1}$) resulting from the shelf

340 waters that contain very high amounts of C_{ant} ($50 \mu\text{mol.kg}^{-1}$). The comparison with other studies confirms that far
341 from the AABW formation sites, contemporary C_{ant} concentrations are not exceeding $16 \mu\text{mol.kg}^{-1}$ on average.
342 Table 3.

343 5.3 C_{ant} trends and variability

344 Comparison of long-term C_{ant} trends in deep and bottom waters of the SO is limited to very few regions where
345 repeated observations are available. To our knowledge, only 3 other studies evaluated the long-term C_{ant} trends in
346 the SO based on more than 5 reoccupations: in the South-western Atlantic (Rios et al., 2012) and in the Weddell
347 Gyre along the Prime meridian section (van Heuven et al., 2011, 2014). Temporal changes of C_T and C_{ant} have
348 also been investigated in other SO regions, but limited to 2 to 4 reoccupations (Williams et al., 2015; Pardo et al.,
349 2017; Murata et al., 2019). Given the C_{ant} variability depicted at our location (Fig. 3a), different trends can be
350 deduced from limited reoccupations. As an example, Murata et al., (2019) evaluated the change in C_{ant} from data
351 collected 17 years apart (1994–1996 and 2012–2013) along a transect around 62° S and found a small increase at
352 our location ($< 5 \mu\text{mol.kg}^{-1}$ around 60° E). This result appears very sensitive to the time of the observation given
353 that we found a minimum in C_{ant} concentrations between 2011 and 2014 (Fig. 3a) associated with a marked C_T
354 minimum (Fig. 3b). In addition, our results show that the detection of C_{ant} trends appears very sensitive to the time
355 period considered (Table 2). As an extreme case, the C_{ant} trend calculated for the period 1987-2004 is $+5.2 \mu\text{mol.kg}^{-1}$
356 $^{\cdot}\text{decade}^{-1}$ (relatively close to the theoretical C_{ant} trend of $+8 \mu\text{mol.kg}^{-1}.\text{decade}^{-1}$), but it reverses to $-3.5 \mu\text{mol.kg}^{-1}$
357 $^{\cdot}\text{decade}^{-1}$ for the period 2004-2018.

358 The long-term C_T trend that we estimated in the LAABW in the eastern Enderby Basin ($2.0 \pm 0.5 \mu\text{mol.kg}^{-1}.\text{decade}^{-1}$)
359 is slightly faster than the C_T trends estimated in the WSBW in the Weddell Gyre: $+1.2 \pm 0.5 \mu\text{mol.kg}^{-1}.\text{decade}^{-1}$
360 over the period 1973-2011 and $+1.6 \pm 1.4 \mu\text{mol.kg}^{-1}.\text{decade}^{-1}$ when restricted to 1996-2011 (van Heuven et al.,
361 2014). Along the SR03 line (south of Tasmania) reoccupied in 1995, 2001, 2008 and 2011, Pardo et al. (2017)
362 calculated a C_T trend of $+2.4 \pm 0.2 \mu\text{mol.kg}^{-1}.\text{decade}^{-1}$ in the AABW, composed of ALBW and RSBW in this sector.
363 This is higher than the C_T trends found at our location and in the Weddell Gyre, but surprisingly, this was not
364 associated with a significant increase in C_{ant} . The C_T trend in AABW along the SR03 section was likely due to the
365 intrusion of old and C_T -rich waters also revealed by an increase in Si concentrations during 1995-2011 (Pardo et
366 al., 2017). This is a clear example of decoupling between C_T and C_{ant} trends in deep and bottom waters as observed
367 at our location in the last decade (Table 2). For C_{ant} , our 40-years trend estimate ($1.4 \pm 0.5 \mu\text{mol.kg}^{-1}.\text{decade}^{-1}$)
368 appears close to the trend reported by Rios et al. (2012) in the south-western Atlantic AABW from 6 reoccupations
369 between 1972 and 2003 ($+1.5 \mu\text{mol.kg}^{-1}.\text{decade}^{-1}$). However, if we limit our result to the period 1978-2002 or
370 1978-2004 (about the same period as in Rios et al., 2012), our trend is much larger ($+3-4 \mu\text{mol.kg}^{-1}.\text{decade}^{-1}$).

371 At our location, the C_{ant} trend over 40 years ($+1.4 \pm 0.5 \mu\text{mol.kg}^{-1}.\text{decade}^{-1}$) explains most of the observed C_T
372 increase ($+2.0 \pm 0.5 \mu\text{mol.kg}^{-1}.\text{decade}^{-1}$). The residual of $+0.4 \mu\text{mol.kg}^{-1}.\text{decade}^{-1}$ reflects changes in natural
373 processes affecting the carbon content (different AABW sources, ventilation, mixing with deep waters,
374 remineralization or carbonates dissolution). Although this is a weak signal, the natural C_T change (C_{nat}) mirrors
375 the observed decrease in O_2 by $-0.8 \pm 0.4 \mu\text{mol.kg}^{-1}.\text{decade}^{-1}$. This O_2 decrease detected in the Enderby Basin
376 appears to be a real feature that was documented at large scale for 1960-2010 in deep SO basins (Schmidtke et al.
377 2017), suggesting that the changes observed at 63° E/ 56.5° S are related to large-scale processes, possibly due to a
378 decrease in AABW formation (Purkey and Johnson, 2012).

379 **5.4 Recent C_{ant} stability**

380 Although most studies suggest a gradual accumulation of C_{ant} in the AABW, our time-series highlights significant
381 multi-annual changes, in particular over the last decade when C_{ant} concentrations were as low as around the year
382 2000 (Fig. 3a) and decoupled from the increase in C_T (Fig. 3b). This result is difficult to interpret because at our
383 location, away from AABW sources (Fig. 1), the temporal variability observed in the LAABW layer can result
384 from many remote processes occurring at the AABW formation sites (such as wind forcing, ventilation, sea-ice
385 melting, thermodynamic, biological activity and air-sea exchanges). Additionally, internal processes during the
386 transport of AABW (such as organic matter remineralization, carbonate dissolution and mixing with surrounding
387 waters) must also be taken into account. The apparent steady C_{ant} feature suggests that AABW found at our location
388 has stored less C_{ant} in recent years. This might be linked to reduced CO_2 uptake in the AABW formation regions,
389 as recognized at large-scale in the SO from the late 1980s to 2001 (Le Quéré et al., 2007; Metzl, 2009; Lenton et
390 al., 2012; Landschützer et al., 2015). This large-scale response in the SO during a positive trend in the Southern
391 Annular Mode (SAM) is mainly associated to stronger winds driven by accelerating greenhouse gas emissions and
392 stratospheric ozone depletion, leading to warming and freshening in the SO (Swart et al., 2018), change in the
393 ventilation of the C_T -rich deep waters and reduced CO_2 uptake (Lenton et al., 2009). The reconstructed $p\text{CO}_2$ fields
394 by Landschützer et al. (2015) suggest that the reduced CO_2 sink in the 1990s is identified at high latitudes in the
395 SO (see Fig. 2a and S9 in Landschützer et al., 2015). However, as opposed to the circumpolar open ocean zone
396 (e.g. Metzl, 2009; Takahashi et al., 2009, 2012; Munro et al., 2015; Fay et al., 2018), the long-term trend of surface
397 $f\text{CO}_2$ and carbon uptake deduced from direct observations are not clearly identified in the seasonal ice zone (SIZ)
398 and shelves around Antarctica, and thus in the AABW formation regions of interest to interpret our results
399 (Laruelle et al., 2018). There, surface $f\text{CO}_2$ data are sparse, especially before 1990, and cruises were mainly
400 conducted in austral summer when the spatio-temporal $f\text{CO}_2$ variability is very large and driven by multiple
401 processes at regional or small scales, such as primary production, sea-ice formation and retreat, and water
402 circulation and mixing. This leads to various estimates of the air-sea CO_2 fluxes around Antarctica depending on
403 the region and period and large uncertainty when attempting to detect long-term trends (Gregor et al., 2018).

404 In particular, in polynyas and AABW formation regions where $f\text{CO}_2$ is low and where katabatic winds prevail,
405 very strong instantaneous CO_2 sink can occur at the local scale (up to $-250 \text{ mmol C.m}^{-2}.\text{d}^{-1}$ in Terra Nova Bay in
406 the Ross Sea according to De Jong and Dunbar, 2017). In the Prydz Bay region where CDBW is formed, recent
407 studies show that surface $f\text{CO}_2$ in austral summer vary over a very large range (150-450 μatm), with the lowest
408 $f\text{CO}_2$ observed in the shelf region generating very strong local CO_2 sink ($-221 \text{ mmol C.m}^{-2}.\text{d}^{-1}$; Roden et al. 2016).
409 The carbon uptake was particularly enhanced near Cape Darnley and coincided with the highest C_{ant} concentrations
410 that Roden et al. (2016) estimated in the dense shelf waters that subduct to form AABW. In the Prydz Bay coastal
411 region, surface $f\text{CO}_2$ values in 1993-1995 were as low as 100 μatm (Gibson and Trull, 1999) leading to a strong
412 local CO_2 uptake of $-30 \text{ mmol C.m}^{-2}.\text{d}^{-1}$ in summer. In addition, Roden et al. (2013) found a large C_T increase over
413 16 years ($+34 \mu\text{mol.kg}^{-1}$) in the Prydz Bay, which is much higher than the anthropogenic signal alone ($+12$
414 $\mu\text{mol.kg}^{-1}$) and likely explained by changes in primary production that would have been stronger in 1994. To our
415 knowledge, this is the only direct observation of decadal C_T change in surface waters in a region of AABW
416 formation (here the Prydz Bay) and it highlights the difficulty not only to evaluate the C_T and C_{ant} long-term trends
417 in these regions but also to separate natural and anthropogenic signals when this water reaches the deep ocean. We
418 attempted to detect long-term changes in CO_2 uptake in this region using the qualified $f\text{CO}_2$ data available in the

419 SOCAT database (Bakker et al., 2016), but our estimates (not shown) were highly uncertain due to very large
420 spatial and temporal variability. To conclude, all previous studies conducted near or in AABW formation sites
421 clearly reveal that these regions are potentially strong carbon sinks, but how the sink changed over the last decades
422 is not yet evaluated, and thus we are not able to certify that the recent C_{ant} stability that we observed in the LAABW
423 at our location is directly linked to the weakening of the carbon sink that was recognized at large-scale in the SO
424 from the 1980s to mid-2000s (Le Quéré et al., 2007; Landschützer et al., 2015).

425 Changes in the accumulation of C_{ant} in AABW could also be directly related to changes in physical processes
426 occurring in AABW formation regions. Decadal decreasing of sea-ice production and melting of sea-ice have been
427 documented in several regions including Cape Darnley polynyas (Tamura et al., 2016; Williams et al., 2016). The
428 consequent changes in Antarctic surface waters properties are transmitted into the deep ocean, notably the well-
429 recognized freshening of the AABW (Rintoul, 2007; Anilkumar et al., 2015). The warming of bottom waters was
430 also documented in the Enderby basin (Couldrey et al., 2013) as well as at a larger scale in all deep SO basins
431 (Purkey and Johnson, 2010; Desbruyères et al., 2016). Associated to a decrease in AABW formation in the 1990s
432 (Purkey and Johnson, 2012), these physical changes could explain the recent stability of C_{ant} concentrations in
433 AABW observed at our location. As AABW from different sources spread and mix with C_T -rich deep waters
434 before reaching our location (Fig. 1), less AABW formation and export would result in an increase in C_T (increase
435 in C_{nat}) not associated with an increase in C_{ant} , and a decrease in O_2 (as observed in recent years in Fig. 3a,b,c).
436 Finally, it is also possible that the LAABW observed in recent years at our location is the result of a larger
437 contribution of older RSBW, ALBW or even WSBW that have lower C_{ant} and O_2 concentrations compared to
438 CDBW formed at Cape Darnley and Prydz Bay.

439 **6 Conclusion**

440 The distribution and evolution of C_{ant} in the bottom layer of the SO are related to complex interactions between
441 climatic forcing, air-sea CO_2 exchange at formation sites, as well as biological and physical processes during
442 AABW circulation. The dataset that we collected regularly in the Enderby basin over the last 20 years (1998-2018)
443 in the frame of the OISO project, together with historical observations obtained in 1978, 1985 and 1987
444 (GEOSECS and INDIGO cruises), allows the investigation of C_{ant} changes in AABW over 40 years in this region.
445 The focus on the AABW variability is made by defining a Lower Antarctic Bottom Water (LAABW) as described
446 in the Section 2.3. Our results suggest that the accumulation of C_{ant} explains most, but not all, of the observed
447 increase in C_T . We also detected a decrease in O_2 that is consistent with the large-scale signal reported by
448 Schmidtke et al. (2017), possibly due to a decrease in AABW formation (Purkey and Johnson, 2012). Our data
449 further indicate rapid anomalies in some periods suggesting that for decadal to long-term estimates care have to
450 be taken when analyzing the change in C_{ant} from data sets collected 10 or 20 years apart (e.g. Williams et al., 2015;
451 Murata et al., 2019). Our results also show different C_{ant} trends on short periods, with a maximum increase of 6.5
452 $\mu\text{mol.kg}^{-1}.\text{decade}^{-1}$ between 1987 and 2004 and an apparent stability in the last 20 years (despite an increase in
453 C_T). This suggests that AABW have stored less C_{ant} in the last decade, but our understanding of the processes that
454 explain this signal is not clear. This might be the result of the reduced CO_2 uptake in the SO in the 1990s (Le Quéré
455 et al., 2007; Landschützer et al., 2015), but this is not yet verified from direct C_T or fCO_2 observations in AABW
456 formation regions due to the lack of winter data and very large variability during summer. This calls for more data

457 collection and investigations in these regions. The apparent stability of C_{ant} in the LAABW since 1998 could also
458 be directly linked to a decrease in AABW formation in the 1990s (Purkey and Johnson, 2012) or a change in the
459 contributions of AABW from different sources, especially in the Prydz Bay region (Williams et al., 2016). In these
460 scenarios, an increased contribution of C_T -rich and O_2 -poor older LCDW along AABW transit would also explain
461 the decoupling between C_{ant} and C_T (increase in C_{nat}) and decrease in O_2 concentrations observed in recent years,
462 even if we tried to isolate this specific feature in our data selection. The decoupling between C_{ant} and C_T is not a
463 unique feature, as it was also reported along the SR03 section between Tasmania and Antarctica, most probably
464 due to advection of C_T -rich waters (Pardo et al., 2017). This highlights the importance of the ocean circulation in
465 influencing the temporal C_T and C_{ant} inventories changes (De Vries et al., 2017) and the need to better separate
466 anthropogenic and natural variability based on time-series observations.

467 The evaluation and understanding of decadal C_{ant} changes in deep and bottom ocean waters are still challenging,
468 as the C_{ant} concentrations remain low compared to C_T measurements accuracy (at best $\pm 2 \mu\text{mol.kg}^{-1}$, Bockmon and
469 Dickson, 2015) and uncertainties of data-based methods ($\pm 6 \mu\text{mol.kg}^{-1}$). Long-term repeated and qualified
470 observations (at least 30 years) are needed to accurately detect and separate the anthropogenic signal from the
471 internal ocean variability; we thus only start to document these trends that should now help to identify
472 shortcomings in models regarding the carbon storage in the deep SO (e.g. Frölicher et al., 2014). As changes in
473 the SO (including warming, freshening, oxygenation/deoxygenation, CO_2 and acidification) are expected to
474 accelerate in the future in response to anthropogenic forcing and climate change (e.g. Heuzé et al., 2014; Hauck et
475 al., 2015; Ito et al., 2015, Yamamoto et al., 2015), it is important to maintain time-series observations to
476 complement the GO-SHIP strategy, and to occupy more regularly other sectors of the SO (Rintoul et al., 2012). In
477 this context, we hope to maintain our observations in the Southern Indian Ocean in the next decade, and with
478 ongoing synthetic products activities such as GLODAPv2 (Olsen et al., 2016, 2019), SOCAT (Bakker et al., 2016)
479 and more recently the SOCCOM project (Williams et al., 2018), to offer a solid database to validate ocean
480 biogeochemical models and coupled climate/carbon models (Russell et al. 2018), and ultimately reduce
481 uncertainties in future climate projections.

482 **Data availability**

483 GEOSECS, INDIGO and OISO 1998-2011 data are publicly available at the Ocean Carbon Data System (OCADS;
484 https://www.nodc.noaa.gov/ocads/oceans/GLODAPv2_2019). OISO original data are available at:
485 www.nodc.noaa.gov/ocads/oceans/RepeatSections/clivar_oiso.html. OISO 2012-2018 will be available in
486 GLODAPv2.2021.

487 **Author contributions**

488 LM, CLM, NM, JF and CM performed the sampling and carried out the measurements of the OISO data. LM
489 prepared the manuscript with contributions from CLM and NM.

490 **Competing interests**

491 The authors declare that they have no conflict of interest.

492 **Acknowledgements**

493 We thank the captains and crew of the R.S.V. Marion Dufresne and the staff at the French Polar Institute (IPEV)
494 for their important contribution to the success of the cruises since 1998. We are also very grateful to all colleagues,
495 students and technicians who helped to obtain the data. We extend our gratitude to P. C. Pardo, S. R. Rintoul and
496 B. Legresy for the discussions during the preparation of the manuscript and to M. K. Shipton for the valuable
497 comments. We thank two anonymous reviewers and the editor M. Hoppema for their comments and constructive
498 suggestions that helped improve the manuscript. The OISO program was and is supported by the French institutes
499 INSU, IPEV and OSU Ecce-Terra and the French program SOERE/Great-Gases. Support from the European
500 Integrated Projects CARBOOCEAN (511176) and CARBOCHANGE (264879) is also acknowledged.

501 **References**

502 Álvarez, M., Lo Monaco, C., Tanhua, T., Yool, A., Oschlies, A., Bullister, J. L., Goyet, C., Metzl, N., Touratier,
503 F., McDonagh, E., and Bryden, H. L.: Estimating the storage of anthropogenic carbon in the subtropical Indian
504 Ocean: a comparison of five different approaches, *Biogeosciences*, 6, 681-703, [https://doi.org/10.5194/bg-6-681-](https://doi.org/10.5194/bg-6-681-2009)
505 [2009](https://doi.org/10.5194/bg-6-681-2009), 2009.

506 Anderson, L. A., and Sarmiento, J. L.: Redfield ratios of remineralization determined by nutrient data analysis,
507 *Global Biogeochemical Cycles*, 8, 65-80, <https://doi.org/10.1029/93gb03318>, 1994.

508 Anderson, L. G., Holby, O., Lindegren, R., and Ohlson, M.: The transport of anthropogenic carbon dioxide into
509 the Weddell Sea, *Journal of Geophysical Research: Oceans*, 96, 16679-16687, <https://doi.org/10.1029/91jc01785>,
510 1991.

511 Anilkumar, N., Chacko, R., Sabu, P., and George, J. V.: Freshening of Antarctic Bottom Water in the Indian Ocean
512 sector of Southern Ocean, *Deep Sea Research Part II: Topical Studies in Oceanography*, 118, 162-169,
513 <https://doi.org/10.1016/j.dsr2.2015.03.009>, 2015.

514 Bakker, D. C. E., Pfeil, B., Landa, C. S., Metzl, N., O'Brien, K. M., Olsen, A., Smith, K., Cosca, C., Harasawa, S.,
515 Jones, S. D., Nakaoka, S., Nojiri, Y., Schuster, U., Steinhoff, T., Sweeney, C., Takahashi, T., Tilbrook, B., Wada,
516 C., Wanninkhof, R., Alin, S. R., Balestrini, C. F., Barbero, L., Bates, N. R., Bianchi, A. A., Bonou, F., Boutin, J.,
517 Bozec, Y., Burger, E. F., Cai, W. J., Castle, R. D., Chen, L., Chierici, M., Currie, K., Evans, W., Featherstone, C.,
518 Feely, R. A., Fransson, A., Goyet, C., Greenwood, N., Gregor, L., Hankin, S., Hardman-Mountford, N. J., Harlay,
519 J., Hauck, J., Hoppema, M., Humphreys, M. P., Hunt, C. W., Huss, B., Ibáñez, J. S. P., Johannessen, T., Keeling,
520 R., Kitidis, V., Körtzinger, A., Kozyr, A., Krasakopoulou, E., Kuwata, A., Landschützer, P., Lauvset, S. K.,
521 Lefèvre, N., Lo Monaco, C., Manke, A., Mathis, J. T., Merlivat, L., Millero, F. J., Monteiro, P. M. S., Munro, D.
522 R., Murata, A., Newberger, T., Omar, A. M., Ono, T., Paterson, K., Pearce, D., Pierrot, D., Robbins, L. L., Saito,
523 S., Salisbury, J., Schlitzer, R., Schneider, B., Schweitzer, R., Sieger, R., Skjelvan, I., Sullivan, K. F., Sutherland,
524 S. C., Sutton, A. J., Tadokoro, K., Telszewski, M., Tuma, M., van Heuven, S. M. A. C., Vandemark, D., Ward, B.,
525 Watson, A. J., and Xu, S.: A multi-decade record of high-quality fCO₂ data in version 3 of the Surface Ocean CO₂
526 Atlas (SOCAT), *Earth Syst. Sci. Data*, 8, 383-413, <https://doi.org/10.5194/essd-8-383-2016>, 2016.

527 Bockmon, E. E., and Dickson, A. G.: An inter-laboratory comparison assessing the quality of seawater carbon
528 dioxide measurements, *Marine Chemistry*, 171, 36-43, <https://doi.org/10.1016/j.marchem.2015.02.002>, 2015.

529 Brewer, P. G.: Direct observation of the oceanic CO₂ increase, *Geophysical Research Letters*, 5, 997-1000,
530 <https://doi.org/10.1029/GL005i012p00997>, 1978.

531 Broecker, W. S.: “NO”, a conservative water-mass tracer, *Earth and Planetary Science Letters*, 23, 100-107,
532 [https://doi.org/10.1016/0012-821X\(74\)90036-3](https://doi.org/10.1016/0012-821X(74)90036-3), 1974.

533 Carmack, E. C., and Foster, T. D.: Circulation and distribution of oceanographic properties near the Filchner Ice
534 Shelf, *Deep Sea Research and Oceanographic Abstracts*, 22, 77-90, [https://doi.org/10.1016/0011-7471\(75\)90097-](https://doi.org/10.1016/0011-7471(75)90097-2)
535 [2](https://doi.org/10.1016/0011-7471(75)90097-2), 1975.

536 Carter, L., McCave, I. N., and Williams, M. J. M.: Chapter 4 Circulation and Water Masses of the Southern Ocean:
537 A Review, in: *Developments in Earth and Environmental Sciences*, edited by: Florindo, F., and Siebert, M.,
538 Elsevier, 85-114, [https://doi.org/10.1016/S1571-9197\(08\)00004-9](https://doi.org/10.1016/S1571-9197(08)00004-9), 2008.

539 Chen, C.-T. A.: On the distribution of anthropogenic CO₂ in the Atlantic and Southern oceans, *Deep Sea Research*
540 *Part A. Oceanographic Research Papers*, 29, 563-580, [https://doi.org/10.1016/0198-0149\(82\)90076-0](https://doi.org/10.1016/0198-0149(82)90076-0), 1982.

541 Chen, G.-T., and Millero, F. J.: Gradual increase of oceanic CO₂, *Nature*, 277, 205-206,
542 <https://doi.org/10.1038/277205a0>, 1979.

543 Chen, T., and Chen, A.: The oceanic anthropogenic CO₂ sink, *Chemosphere*, 27, 1041-1064,
544 [https://doi.org/10.1016/0045-6535\(93\)90067-F](https://doi.org/10.1016/0045-6535(93)90067-F), 1993.

545 Coverly, S. C., Aminot, A., and R. K  rouel, 2009. Nutrients in Seawater Using Segmented Flow Analysis, In:
546 *Practical Guidelines for the Analysis of Seawater*, Edited by: Oliver Wurl, CRC Press,
547 <https://doi.org/10.1201/9781420073072>, 2009.

548 De Baar, H. J. W.: Options for enhancing the storage of carbon dioxide in the oceans: A review, *Energy Conversion*
549 *and Management*, 33, 635-642, [https://doi.org/10.1016/0196-8904\(92\)90066-6](https://doi.org/10.1016/0196-8904(92)90066-6), 1992.

550 DeJong, H. B., and Dunbar, R. B.: Air-Sea CO₂ Exchange in the Ross Sea, Antarctica, *Journal of Geophysical*
551 *Research: Oceans*, 122, 8167-8181, <https://doi.org/10.1002/2017JC012853>, 2017.

552 Desbruy  res, D. G., Purkey, S. G., McDonagh, E. L., Johnson, G. C., and King, B. A.: Deep and abyssal ocean
553 warming from 35 years of repeat hydrography, *Geophysical Research Letters*, 43, 10356-10365,
554 <https://doi.org/10.1002/2016GL070413>, 2016.

555 DeVries, T., Holzer, M., and Primeau, F.: Recent increase in oceanic carbon uptake driven by weaker upper-ocean
556 overturning, *Nature*, 542, 215-218, <https://doi.org/10.1038/nature21068>, 2017.

557 Edmond, J. M.: High precision determination of titration alkalinity and total carbon dioxide content of sea water
558 by potentiometric titration, *Deep Sea Research and Oceanographic Abstracts*, 17, 737-750,
559 [https://doi.org/10.1016/0011-7471\(70\)90038-0](https://doi.org/10.1016/0011-7471(70)90038-0), 1970.

560 Fahrbach, E., Rohardt, G., Schröder, M., and Strass, V.: Transport and structure of the Weddell Gyre, *Ann.*
561 *Geophys.*, 12, 840-855, <https://doi.org/10.1007/s00585-994-0840-7>, 1994.

562 Fay, A. R., Lovenduski, N. S., McKinley, G. A., Munro, D. R., Sweeney, C., Gray, A. R., Landschützer, P.,
563 Stephens, B. B., Takahashi, T., and Williams, N.: Utilizing the Drake Passage Time-series to understand variability
564 and change in subpolar Southern Ocean pCO₂, *Biogeosciences*, 15, 3841-3855, [https://doi.org/10.5194/bg-15-](https://doi.org/10.5194/bg-15-3841-2018)
565 [3841-2018](https://doi.org/10.5194/bg-15-3841-2018), 2018.

566 Frölicher, T. L., Sarmiento, J. L., Paynter, D. J., Dunne, J. P., Krasting, J. P., and Winton, M.: Dominance of the
567 Southern Ocean in Anthropogenic Carbon and Heat Uptake in CMIP5 Models, *Journal of Climate*, 28, 862-886,
568 <https://doi.org/10.1175/jcli-d-14-00117.1>, 2015.

569 Fukamachi, Y., Wakatsuchi, M., Taira, K., Kitagawa, S., Ushio, S., Takahashi, A., Oikawa, K., Furukawa, T.,
570 Yoritaka, H., Fukuchi, M., and Yamanouchi, T.: Seasonal variability of bottom water properties off Adélie Land,
571 Antarctica, *Journal of Geophysical Research: Oceans*, 105, 6531-6540, <https://doi.org/10.1029/1999JC900292>,
572 2000.

573 Fukamachi, Y., Rintoul, S. R., Church, J. A., Aoki, S., Sokolov, S., Rosenberg, M. A., and Wakatsuchi, M.: Strong
574 export of Antarctic Bottom Water east of the Kerguelen plateau, *Nature Geoscience*, 3, 327-331,
575 <https://doi.org/10.1038/ngeo842>, 2010.

576 Gattuso, J.-P. and Hansson, L.: *Ocean Acidification*, Oxford University Press, Oxford, New York., 2011.

577 Gibson, J. A. E., and Trull, T. W.: Annual cycle of fCO₂ under sea-ice and in open water in Prydz Bay, East
578 Antarctica, *Marine Chemistry*, 66, 187-200, [https://doi.org/10.1016/S0304-4203\(99\)00040-7](https://doi.org/10.1016/S0304-4203(99)00040-7), 1999.

579 Gordon, A. L.: Bottom Water Formation, in *Encyclopedia of Ocean Sciences*, pp. 334–340, Elsevier., 2001.

580 Gordon, A. L., Orsi, A. H., Muench, R., Huber, B. A., Zambianchi, E., and Visbeck, M.: Western Ross Sea
581 continental slope gravity currents, *Deep Sea Research Part II: Topical Studies in Oceanography*, 56, 796-817,
582 <https://doi.org/10.1016/j.dsr2.2008.10.037>, 2009.

583 Gordon, A. L., Huber, B., McKee, D., and Visbeck, M.: A seasonal cycle in the export of bottom water from the
584 Weddell Sea, *Nature Geoscience*, 3, 551-556, <https://doi.org/10.1038/ngeo916>, 2010.

585 Gordon, A. L., Huber, B. A., and Busecke, J.: Bottom water export from the western Ross Sea, 2007 through 2010,
586 *Geophysical Research Letters*, 42, 5387-5394, <https://doi.org/10.1002/2015GL064457>, 2015.

587 Goyet, C., Adams, R., and Eiseheid, G.: Observations of the CO₂ system properties in the tropical Atlantic Ocean,
588 *Marine Chemistry*, 60, 49-61, [https://doi.org/10.1016/S0304-4203\(97\)00081-9](https://doi.org/10.1016/S0304-4203(97)00081-9), 1998.

589 Gregor, L., Kok, S., and Monteiro, P. M. S.: Interannual drivers of the seasonal cycle of CO₂ in the Southern
590 Ocean, *Biogeosciences*, 15, 2361-2378, <https://doi.org/10.5194/bg-15-2361-2018>, 2018.

591 Gruber, N.: Anthropogenic CO₂ in the Atlantic Ocean, *Global Biogeochemical Cycles*, 12, 165-191,
592 <https://doi.org/10.1029/97GB03658>, 1998.

593 Gruber, N., Gloor, M., Mikaloff Fletcher, S. E., Doney, S. C., Dutkiewicz, S., Follows, M. J., Gerber, M., Jacobson,
594 A. R., Joos, F., Lindsay, K., Menemenlis, D., Mouchet, A., Müller, S. A., Sarmiento, J. L., and Takahashi, T.:
595 Oceanic sources, sinks, and transport of atmospheric CO₂, *Global Biogeochemical Cycles*, 23,
596 <https://doi.org/10.1029/2008GB003349>, 2009.

597 Gruber, N., Clement, D., Carter, B. R., Feely, R. A., van Heuven, S., Hoppema, M., Ishii, M., Key, R. M., Kozyr,
598 A., Lauvset, S. K., Lo Monaco, C., Mathis, J. T., Murata, A., Olsen, A., Perez, F. F., Sabine, C. L., Tanhua, T.,
599 and Wanninkhof, R.: The oceanic sink for anthropogenic CO₂; from 1994 to 2007, *Science*, 363, 1193-1199,
600 <https://doi.org/10.1126/science.aau5153>, 2019a.

601 Gruber, N., Landschützer, P., and Lovenduski, N. S.: The Variable Southern Ocean Carbon Sink, *Annual Review*
602 *of Marine Science*, 11, 159-186, <https://doi.org/10.1146/annurev-marine-121916-063407>, 2019b.

603 Hall, T. M., Haine, T. W. N., and Waugh, D. W.: Inferring the concentration of anthropogenic carbon in the ocean
604 from tracers, *Global Biogeochemical Cycles*, 16, 1131, <https://doi.org/10.1029/2001GB001835>, 2002.

605 Hauck, J., Völker, C., Wolf-Gladrow, D. A., Laufkötter, C., Vogt, M., Aumont, O., Bopp, L., Buitenhuis, E. T.,
606 Doney, S. C., Dunne, J., Gruber, N., Hashioka, T., John, J., Quéré, C. L., Lima, I. D., Nakano, H., Séférian, R.,
607 and Totterdell, I.: On the Southern Ocean CO₂ uptake and the role of the biological carbon pump in the 21st
608 century, *Global Biogeochemical Cycles*, 29, 1451-1470, <https://doi.org/10.1002/2015GB005140>, 2015.

609 Heuzé, C., Heywood, K. J., Stevens, D. P., and Ridley, J. K.: Changes in Global Ocean Bottom Properties and
610 Volume Transports in CMIP5 Models under Climate Change Scenarios*, *Journal of Climate*, 28, 2917-2944,
611 <https://doi.org/10.1175/JCLI-D-14-00381.1>, 2015.

612 Heywood, K. J., Sparrow, M. D., Brown, J., and Dickson, R. R.: Frontal structure and Antarctic Bottom Water
613 flow through the Princess Elizabeth Trough, *Antarctica, Deep Sea Research Part I: Oceanographic Research*
614 *Papers*, 46, 1181-1200, [https://doi.org/10.1016/S0967-0637\(98\)00108-3](https://doi.org/10.1016/S0967-0637(98)00108-3), 1999.

615 Ito, T., Bracco, A., Deutsch, C., Frenzel, H., Long, M., and Takano, Y.: Sustained growth of the Southern Ocean
616 carbon storage in a warming climate, *Geophysical Research Letters*, 42, 4516-4522,
617 <https://doi.org/10.1002/2015GL064320>, 2015.

618 Jabaud-Jan, A., Metzl, N., Brunet, C., Poisson, A., and Schauer, B.: Interannual variability of the carbon dioxide
619 system in the southern Indian Ocean (20°S–60°S): The impact of a warm anomaly in austral summer 1998, *Global*
620 *Biogeochemical Cycles*, 18, GB1042, <https://doi.org/10.1029/2002GB002017>, 2004.

621 Jiang, L.-Q., Carter, B. R., Feely, R. A., Lauvset, S. K., and Olsen, A.: Surface ocean pH and buffer capacity: past,
622 present and future, *Scientific Reports*, 9, 18624, <https://doi.org/10.1038/s41598-019-55039-4>, 2019.

623 Johnson, G. C.: Quantifying Antarctic Bottom Water and North Atlantic Deep Water volumes, *Journal of*
624 *Geophysical Research: Oceans*, 113, C05027, <https://doi.org/10.1029/2007JC004477>, 2008.

625 Johnson, G. C., Purkey, S. G., and Bullister, J. L.: Warming and Freshening in the Abyssal Southeastern Indian
626 Ocean*, *Journal of Climate*, 21, 5351-5363, <https://doi.org/10.1175/2008JCLI2384.1>, 2008.

627 Kerr, R., Goyet, C., da Cunha, L. C., Orselli, I. B. M., Lencina-Avila, J. M., Mendes, C. R. B., Carvalho-Borges,
628 M., Mata, M. M., and Tavano, V. M.: Carbonate system properties in the Gerlache Strait, Northern Antarctic
629 Peninsula (February 2015): II. Anthropogenic CO₂ and seawater acidification, *Deep Sea Research Part II: Topical*
630 *Studies in Oceanography*, 149, 182-192, <https://doi.org/10.1016/j.dsr2.2017.07.007>, 2018.

631 Key, R. M., Kozyr, A., Sabine, C. L., Lee, K., Wanninkhof, R., Bullister, J. L., Feely, R. A., Millero, F. J., Mordy,
632 C., and Peng, T. H.: A global ocean carbon climatology: Results from Global Data Analysis Project (GLODAP),
633 *Global Biogeochemical Cycles*, 18, GB4031, <https://doi.org/10.1029/2004GB002247>, 2004.

634 Key, R. M., Tanhua, T., Olsen, A., Hoppema, M., Jutterström, S., Schirnick, C., van Heuven, S., Kozyr, A., Lin,
635 X., Velo, A., Wallace, D. W. R., and Mintrop, L.: The CARINA data synthesis project: introduction and overview,
636 *Earth Syst. Sci. Data*, 2, 105-121, <https://doi.org/10.5194/essd-2-105-2010>, 2010.

637 Key, R. M., Olsen, A., Van Heuven, S., Lauvset, S. K., Velo, A., Lin, X., Schirnick, C., Kozyr, A., Tanhua, T.,
638 Hoppema, M., Jutterstrom, S., Steinfeldt, R., Jeansson, E., Ishi, M., Perez, F. F. and Suzuki, T.: Global Ocean Data
639 Analysis Project, Version 2 (GLODAPv2), ORNL/CDIAC-162, ND-P093,
640 doi:[10.3334/CDIAC/OTG.NDP093_GLODAPv2](https://doi.org/10.3334/CDIAC/OTG.NDP093_GLODAPv2), 2015.

641 Khatiwala, S., Primeau, F., and Hall, T.: Reconstruction of the history of anthropogenic CO₂ concentrations in the
642 ocean, *Nature*, 462, 346-349, <https://doi.org/10.1038/nature08526>, 2009.

643 Khatiwala, S., Tanhua, T., Mikaloff Fletcher, S., Gerber, M., Doney, S. C., Graven, H. D., Gruber, N., McKinley,
644 G. A., Murata, A., Ríos, A. F., and Sabine, C. L.: Global ocean storage of anthropogenic carbon, *Biogeosciences*,
645 10, 2169-2191, <https://doi.org/10.5194/bg-10-2169-2013>, 2013.

646 Körtzinger, A., Mintrop, L., and Duinker, J. C.: On the penetration of anthropogenic CO₂ into the North Atlantic
647 Ocean, *Journal of Geophysical Research: Oceans*, 103, 18681-18689, <https://doi.org/10.1029/98JC01737>, 1998.

648 Körtzinger, A., Rhein, M., and Mintrop, L.: Anthropogenic CO₂ and CFCs in the North Atlantic Ocean - A
649 comparison of man-made tracers, *Geophysical Research Letters*, 26, 2065-2068,
650 <https://doi.org/10.1029/1999GL900432>, 1999.

651 Körtzinger, A., Hedges, J. I., and Quay, P. D.: Redfield ratios revisited: Removing the biasing effect of
652 anthropogenic CO₂, *Limnology and Oceanography*, 46, 964-970, <https://doi.org/10.4319/lo.2001.46.4.0964>, 2001.

653 Landschützer, P., Gruber, N., Haumann, F. A., Rödenbeck, C., Bakker, D. C. E., van Heuven, S., Hoppema, M.,
654 Metzl, N., Sweeney, C., Takahashi, T., Tilbrook, B., and Wanninkhof, R.: The reinvigoration of the Southern
655 Ocean carbon sink, *Science*, 349, 1221-1224, <https://doi.org/10.1126/science.aab2620>, 2015.

656 Laruelle, G. G., Cai, W.-J., Hu, X., Gruber, N., Mackenzie, F. T., and Regnier, P.: Continental shelves as a variable
657 but increasing global sink for atmospheric carbon dioxide, *Nature Communications*, 9, 454,
658 <https://doi.org/10.1038/s41467-017-02738-z>, 2018.

659 Le Quéré, C., Rödenbeck, C., Buitenhuis, E. T., Conway, T. J., Langenfelds, R., Gomez, A., Labuschagne, C.,
660 Ramonet, M., Nakazawa, T., Metzl, N., Gillett, N., and Heimann, M.: Saturation of the Southern Ocean CO₂; Sink
661 Due to Recent Climate Change, *Science*, 316, 1735-1738, <https://doi.org/10.1126/science.1136188>, 2007.

662 Le Quéré, C., Andrew, R. M., Friedlingstein, P., Sitch, S., Hauck, J., Pongratz, J., Pickers, P. A., Korsbakken, J.
663 I., Peters, G. P., Canadell, J. G., Arneeth, A., Arora, V. K., Barbero, L., Bastos, A., Bopp, L., Chevallier, F., Chini,
664 L. P., Ciais, P., Doney, S. C., Gkritzalis, T., Goll, D. S., Harris, I., Haverd, V., Hoffman, F. M., Hoppema, M.,
665 Houghton, R. A., Hurtt, G., Ilyina, T., Jain, A. K., Johannessen, T., Jones, C. D., Kato, E., Keeling, R. F.,
666 Goldewijk, K. K., Landschützer, P., Lefèvre, N., Lienert, S., Liu, Z., Lombardozzi, D., Metzl, N., Munro, D. R.,
667 Nabel, J. E. M. S., Nakaoka, S., Neill, C., Olsen, A., Ono, T., Patra, P., Peregon, A., Peters, W., Peylin, P., Pfeil,
668 B., Pierrot, D., Poulter, B., Rehder, G., Resplandy, L., Robertson, E., Rocher, M., Rödenbeck, C., Schuster, U.,
669 Schwinger, J., Séférian, R., Skjelvan, I., Steinhoff, T., Sutton, A., Tans, P. P., Tian, H., Tilbrook, B., Tubiello, F.
670 N., van der Laan-Luijkx, I. T., van der Werf, G. R., Viovy, N., Walker, A. P., Wiltshire, A. J., Wright, R., Zaehle,
671 S., and Zheng, B.: Global Carbon Budget 2018, *Earth Syst. Sci. Data*, 10, 2141-2194, <https://doi.org/10.5194/essd-10-2141-2018>, 2018.

672

673 Lenton, A., Metzl, N., Takahashi, T., Kuchinke, M., Matear, R. J., Roy, T., Sutherland, S. C., Sweeney, C., and
674 Tilbrook, B.: The observed evolution of oceanic pCO₂ and its drivers over the last two decades, *Global
675 Biogeochemical Cycles*, 26, GB2021, <https://doi.org/10.1029/2011GB004095>, 2012.

676

677

678 Lo Monaco, C., Goyet, C., Metzl, N., Poisson, A., and Touratier, F.: Distribution and inventory of anthropogenic
679 CO₂ in the Southern Ocean: Comparison of three data-based methods, *Journal of Geophysical Research: Oceans*,
680 110, C09S02, <https://doi.org/10.1029/2004JC002571>, 2005a.

681

682

683 Lo Monaco, C., Metzl, N., Poisson, A., Brunet, C., and Schauer, B.: Anthropogenic CO₂ in the Southern Ocean:
684 Distribution and inventory at the Indian-Atlantic boundary (World Ocean Circulation Experiment line I6), *Journal
685 of Geophysical Research: Oceans*, 110, C06010, <https://doi.org/10.1029/2004JC002643>, 2005b.

686

687 Lo Monaco, C., Álvarez, M., Key, R. M., Lin, X., Tanhua, T., Tilbrook, B., Bakker, D. C. E., van Heuven, S.,
688 Hoppema, M., Metzl, N., Ríos, A. F., Sabine, C. L., and Velo, A.: Assessing the internal consistency of the
689 CARINA database in the Indian sector of the Southern Ocean, *Earth Syst. Sci. Data*, 2, 51-70,
690 <https://doi.org/10.5194/essd-2-51-2010>, 2010.

691

692

693

694

695

696

697

698

699

700

701

702

703

704

705

706

707

708

709

710

711

712

713

714

715

716

717

718

719

720

721

722

723

724

725

726

727

728

729

730

731

732

733

734

735

736

737

738

739

740

741

742

743

744

745

746

747

748

749

750

751

752

753

754

755

756

757

758

759

760

761

762

763

764

765

766

767

768

769

770

771

772

773

774

775

776

777

778

779

780

781

782

783

784

785

786

787

788

789

790

791

792

793

794

795

796

797

798

799

800

801

802

803

804

805

806

807

808

809

810

811

812

813

814

815

816

817

818

819

820

821

822

823

824

825

826

827

828

829

830

831

832

833

834

835

836

837

838

839

840

841

842

843

844

845

846

847

848

849

850

851

852

853

854

855

856

857

858

859

860

861

862

863

864

865

866

867

868

869

870

871

872

873

874

875

876

877

878

879

880

881

882

883

884

885

886

887

888

889

890

891

892

893

894

895

896

897

898

899

900

901

902

903

904

905

906

907

908

909

910

911

912

913

914

915

916

917

918

919

920

921

922

923

924

925

926

927

928

929

930

931

932

933

934

935

936

937

938

939

940

941

942

943

944

945

946

947

948

949

950

951

952

953

954

955

956

957

958

959

960

961

962

963

964

965

966

967

968

969

970

971

972

973

974

975

976

977

978

979

980

981

982

983

984

985

986

987

988

989

990

991

992

993

994

995

996

997

998

999

1000

688 Marshall, J., and Speer, K.: Closure of the meridional overturning circulation through Southern Ocean upwelling,
689 Nature Geoscience, 5, 171-180, <https://doi.org/10.1038/ngeo1391>, 2012.

690 Matear, R. J.: Effects of numerical advection schemes and eddy parameterizations on ocean ventilation and oceanic
691 anthropogenic CO₂ uptake, Ocean Modelling, 3, 217-248, [https://doi.org/10.1016/S1463-5003\(01\)00010-5](https://doi.org/10.1016/S1463-5003(01)00010-5), 2001.

692 McKee, D. C., Yuan, X., Gordon, A. L., Huber, B. A., and Dong, Z.: Climate impact on interannual variability of
693 Weddell Sea Bottom Water, Journal of Geophysical Research: Oceans, 116, C05020,
694 <https://doi.org/10.1029/2010JC006484>, 2011.

695 McNeil, B. I., Matear, R. J., Key, R. M., Bullister, J. L., and Sarmiento, J. L.: Anthropogenic CO₂ Uptake by the
696 Ocean Based on the Global Chlorofluorocarbon Data Set, Science, 299, 235-239,
697 <https://doi.org/10.1126/science.1077429>, 2003.

698 Meijers, A. J. S., Klocker, A., Bindoff, N. L., Williams, G. D., and Marsland, S. J.: The circulation and water
699 masses of the Antarctic shelf and continental slope between 30 and 80°E, Deep Sea Research Part II: Topical
700 Studies in Oceanography, 57, 723-737, <https://doi.org/10.1016/j.dsr2.2009.04.019>, 2010.

701 Menezes, V. V., Macdonald, A. M., and Schatzman, C.: Accelerated freshening of Antarctic Bottom Water over
702 the last decade in the Southern Indian Ocean, Science Advances, 3, e1601426,
703 <https://doi.org/10.1126/sciadv.1601426>, 2017.

704 Metzl, N., Brunet, C., Jabaud-Jan, A., Poisson, A., and Schauer, B.: Summer and winter air–sea CO₂ fluxes in the
705 Southern Ocean, Deep Sea Research Part I: Oceanographic Research Papers, 53, 1548-1563,
706 <https://doi.org/10.1016/j.dsr.2006.07.006>, 2006.

707 Metzl, N.: Decadal increase of oceanic carbon dioxide in Southern Indian Ocean surface waters (1991–2007),
708 Deep Sea Research Part II: Topical Studies in Oceanography, 56, 607-619,
709 <https://doi.org/10.1016/j.dsr2.2008.12.007>, 2009.

710 Munro, D. R., Lovenduski, N. S., Takahashi, T., Stephens, B. B., Newberger, T., and Sweeney, C.: Recent evidence
711 for a strengthening CO₂ sink in the Southern Ocean from carbonate system measurements in the Drake Passage
712 (2002–2015), Geophysical Research Letters, 42, 7623-7630, <https://doi.org/10.1002/2015GL065194>, 2015.

713 Murata, A., Kumamoto, Y.-i., and Sasaki, K.-i.: Decadal-Scale Increases of Anthropogenic CO₂ in Antarctic
714 Bottom Water in the Indian and Western Pacific Sectors of the Southern Ocean, Geophysical Research Letters,
715 46, 833-841, <https://doi.org/10.1029/2018GL080604>, 2019.

716 Ohshima, K. I., Fukamachi, Y., Williams, G. D., Nihashi, S., Roquet, F., Kitade, Y., Tamura, T., Hirano, D.,
717 Herraiz-Borreguero, L., Field, I., Hindell, M., Aoki, S., and Wakatsuchi, M.: Antarctic Bottom Water production
718 by intense sea-ice formation in the Cape Darnley polynya, Nature Geoscience, 6, 235-240,
719 <https://doi.org/10.1038/ngeo1738>, 2013.

720 Olsen, A., Key, R. M., van Heuven, S., Lauvset, S. K., Velo, A., Lin, X., Schirnack, C., Kozyr, A., Tanhua, T.,
721 Hoppema, M., Jutterström, S., Steinfeldt, R., Jeansson, E., Ishii, M., Pérez, F. F., and Suzuki, T.: The Global Ocean
722 Data Analysis Project version 2 (GLODAPv2) – an internally consistent data product for the world ocean, *Earth*
723 *Syst. Sci. Data*, 8, 297-323, <https://doi.org/10.5194/essd-8-297-2016>, 2016.

724 Olsen, A., Lange, N., Key, R. M., Tanhua, T., Álvarez, M., Becker, S., Bittig, H. C., Carter, B. R., Cotrim da
725 Cunha, L., Feely, R. A., van Heuven, S., Hoppema, M., Ishii, M., Jeansson, E., Jones, S. D., Jutterström, S.,
726 Karlsen, M. K., Kozyr, A., Lauvset, S. K., Lo Monaco, C., Murata, A., Pérez, F. F., Pfeil, B., Schirnack, C.,
727 Steinfeldt, R., Suzuki, T., Telszewski, M., Tilbrook, B., Velo, A., and Wanninkhof, R.: GLODAPv2.2019 – an
728 update of GLODAPv2, *Earth Syst. Sci. Data*, 11, 1437-1461, <https://doi.org/10.5194/essd-11-1437-2019>, 2019.

729 Orr, J. C., Maier-Reimer, E., Mikolajewicz, U., Monfray, P., Sarmiento, J. L., Toggweiler, J. R., Taylor, N. K.,
730 Palmer, J., Gruber, N., Sabine, C. L., Le Quéré, C., Key, R. M., and Boutin, J.: Estimates of anthropogenic carbon
731 uptake from four three-dimensional global ocean models, *Global Biogeochemical Cycles*, 15, 43-60,
732 <https://doi.org/10.1029/2000GB001273>, 2001.

733 Orr, J. C., Fabry, V. J., Aumont, O., Bopp, L., Doney, S. C., Feely, R. A., Gnanadesikan, A., Gruber, N., Ishida,
734 A., Joos, F., Key, R. M., Lindsay, K., Maier-Reimer, E., Matear, R., Monfray, P., Mouchet, A., Najjar, R. G.,
735 Plattner, G.-K., Rodgers, K. B., Sabine, C. L., Sarmiento, J. L., Schlitzer, R., Slater, R. D., Totterdell, I. J., Weirig,
736 M.-F., Yamanaka, Y., and Yool, A.: Anthropogenic ocean acidification over the twenty-first century and its impact
737 on calcifying organisms, *Nature*, 437, 681-686, <https://doi.org/10.1038/nature04095>, 2005.

738 Orsi, A. H., Johnson, G. C., and Bullister, J. L.: Circulation, mixing, and production of Antarctic Bottom Water,
739 *Progress in Oceanography*, 43, 55-109, [https://doi.org/10.1016/S0079-6611\(99\)00004-X](https://doi.org/10.1016/S0079-6611(99)00004-X), 1999.

740 Pardo, P. C., Pérez, F. F., Khatiwala, S., and Ríos, A. F.: Anthropogenic CO₂ estimates in the Southern Ocean:
741 Storage partitioning in the different water masses, *Progress in Oceanography*, 120, 230-242,
742 <https://doi.org/10.1016/j.pocean.2013.09.005>, 2014.

743 Pardo, P. C., Tilbrook, B., Langlais, C., Trull, T. W., and Rintoul, S. R.: Carbon uptake and biogeochemical change
744 in the Southern Ocean, south of Tasmania, *Biogeosciences*, 14, 5217-5237, [https://doi.org/10.5194/bg-14-5217-](https://doi.org/10.5194/bg-14-5217-2017)
745 [2017](https://doi.org/10.5194/bg-14-5217-2017), 2017.

746 Poisson, A., and Chen, C.-T. A.: Why is there little anthropogenic CO₂ in the Antarctic bottom water?, *Deep Sea*
747 *Research Part A. Oceanographic Research Papers*, 34, 1255-1275, [https://doi.org/10.1016/0198-0149\(87\)90075-](https://doi.org/10.1016/0198-0149(87)90075-6)
748 [6](https://doi.org/10.1016/0198-0149(87)90075-6), 1987.

749 Purkey, S. G., and Johnson, G. C.: Warming of Global Abyssal and Deep Southern Ocean Waters between the
750 1990s and 2000s: Contributions to Global Heat and Sea Level Rise Budgets*, *Journal of Climate*, 23, 6336-6351,
751 <https://doi.org/10.1175/2010JCLI3682.1>, 2010.

752 Purkey, S. G., and Johnson, G. C.: Global Contraction of Antarctic Bottom Water between the 1980s and 2000s*,
753 *Journal of Climate*, 25, 5830-5844, <https://doi.org/10.1175/JCLI-D-11-00612.1>, 2012.

754 Ridgwell, A., and Zeebe, R. E.: The role of the global carbonate cycle in the regulation and evolution of the Earth
755 system, *Earth and Planetary Science Letters*, 234, 299-315, <https://doi.org/10.1016/j.epsl.2005.03.006>, 2005.

756 Rintoul, S. R.: Rapid freshening of Antarctic Bottom Water formed in the Indian and Pacific oceans, *Geophysical
757 Research Letters*, 34, L06606, <https://doi.org/10.1029/2006GL028550>, 2007.

758 Rintoul, S.R., Sparrow, M., Meredith, M.P., Wadley, V., Speer, K., Hofmann, E., Summerhayes, C., Urban, E.,
759 and Bellerby, R.: The Southern Ocean Observing System: Initial Science and Implementation Strategy. Scientific
760 Committee on Antarctic Research/Scientific Committee on Oceanic Research, 74 pp., 2012.

761 Ríos, A. F., Velo, A., Pardo, P. C., Hoppema, M., and Pérez, F. F.: An update of anthropogenic CO₂ storage rates
762 in the western South Atlantic basin and the role of Antarctic Bottom Water, *Journal of Marine Systems*, 94, 197-
763 203, <https://doi.org/10.1016/j.jmarsys.2011.11.023>, 2012.

764 Robertson, R., Visbeck, M., Gordon, A. L., and Fahrback, E.: Long-term temperature trends in the deep waters of
765 the Weddell Sea, *Deep Sea Research Part II: Topical Studies in Oceanography*, 49, 4791-4806,
766 [https://doi.org/10.1016/S0967-0645\(02\)00159-5](https://doi.org/10.1016/S0967-0645(02)00159-5), 2002.

767 Rodehacke, C. B., Hellmer, H. H., Beckmann, A., and Roether, W.: Formation and spreading of Antarctic deep
768 and bottom waters inferred from a chlorofluorocarbon (CFC) simulation, *Journal of Geophysical Research:
769 Oceans*, 112, C09001, <https://doi.org/10.1029/2006JC003884>, 2007.

770 Roden, N. P., Shadwick, E. H., Tilbrook, B., and Trull, T. W.: Annual cycle of carbonate chemistry and decadal
771 change in coastal Prydz Bay, East Antarctica, *Marine Chemistry*, 155, 135-147,
772 <https://doi.org/10.1016/j.marchem.2013.06.006>, 2013.

773 Roden, N. P., Tilbrook, B., Trull, T. W., Virtue, P., and Williams, G. D.: Carbon cycling dynamics in the seasonal
774 sea-ice zone of East Antarctica, *Journal of Geophysical Research: Oceans*, 121, 8749-8769,
775 <https://doi.org/10.1002/2016JC012008>, 2016.

776 Russell, J. L., Kamenkovich, I., Bitz, C., Ferrari, R., Gille, S. T., Goodman, P. J., Hallberg, R., Johnson, K.,
777 Khazmutdinova, K., Marinov, I., Mazloff, M., Riser, S., Sarmiento, J. L., Speer, K., Talley, L. D., and Wanninkhof,
778 R.: Metrics for the Evaluation of the Southern Ocean in Coupled Climate Models and Earth System Models,
779 *Journal of Geophysical Research: Oceans*, 123, 3120-3143, <https://doi.org/10.1002/2017JC013461>, 2018.

780 Sabine, C. L., Key, R. M., Johnson, K. M., Millero, F. J., Poisson, A., Sarmiento, J. L., Wallace, D. W. R., and
781 Winn, C. D.: Anthropogenic CO₂ inventory of the Indian Ocean, *Global Biogeochemical Cycles*, 13, 179-198,
782 <https://doi.org/10.1029/1998GB900022>, 1999.

783 Sabine, C. L., Feely, R. A., Gruber, N., Key, R. M., Lee, K., Bullister, J. L., Wanninkhof, R., Wong, C. S., Wallace,
784 D. W. R., Tilbrook, B., Millero, F. J., Peng, T.-H., Kozyr, A., Ono, T., and Rios, A. F.: The Oceanic Sink for
785 Anthropogenic CO₂, *Science*, 305, 367-371, <https://doi.org/10.1126/science.1097403>, 2004.

786 Sandrini, S., Ait-Ameur, N., Rivaro, P., Massolo, S., Touratier, F., Tositti, L., and Goyet, C.: Anthropogenic carbon
787 distribution in the Ross Sea, Antarctica, *Antarctic Science*, 19, 395-407,
788 <https://doi.org/10.1017/S0954102007000405>, 2007.

789 Schlitzer, R., Ocean data view, <http://odv.awi.de>, 2019.

790 Schmidtko, S., Stramma, L., and Visbeck, M.: Decline in global oceanic oxygen content during the past five
791 decades, *Nature*, 542, 335-339, <https://doi.org/10.1038/nature21399>, 2017.

792 Shadwick, E. H., Rintoul, S. R., Tilbrook, B., Williams, G. D., Young, N., Fraser, A. D., Marchant, H., Smith, J.,
793 and Tamura, T.: Glacier tongue calving reduced dense water formation and enhanced carbon uptake, *Geophysical*
794 *Research Letters*, 40, 904-909, <https://doi.org/10.1002/grl.50178>, 2013.

795 Shadwick, E. H., Tilbrook, B., and Williams, G. D.: Carbonate chemistry in the Mertz Polynya (East Antarctica):
796 Biological and physical modification of dense water outflows and the export of anthropogenic CO₂, *Journal of*
797 *Geophysical Research: Oceans*, 119, 1-14, <https://doi.org/10.1002/2013JC009286>, 2014.

798 Siegenthaler, U., and Sarmiento, J. L.: Atmospheric carbon dioxide and the ocean, *Nature*, 365, 119-125,
799 <https://doi.org/10.1038/365119a0>, 1993.

800 Smith, N. and Treguer, P.: *Physical and Chemical Oceanography in the Vicinity of Prydz Bay, Antarctica*, edited
801 by S. Z. ElSayed, Cambridge Univ Press, Cambridge., 1994.

802 Takahashi, T., Sutherland, S. C., Wanninkhof, R., Sweeney, C., Feely, R. A., Chipman, D. W., Hales, B.,
803 Friederich, G., Chavez, F., Sabine, C., Watson, A., Bakker, D. C. E., Schuster, U., Metzl, N., Yoshikawa-Inoue,
804 H., Ishii, M., Midorikawa, T., Nojiri, Y., Körtzinger, A., Steinhoff, T., Hoppema, M., Olafsson, J., Arnarson, T.
805 S., Tilbrook, B., Johannessen, T., Olsen, A., Bellerby, R., Wong, C. S., Delille, B., Bates, N. R., and de Baar, H.
806 J. W.: Climatological mean and decadal change in surface ocean pCO₂, and net sea-air CO₂ flux over the global
807 oceans, *Deep Sea Research Part II: Topical Studies in Oceanography*, 56, 554-577,
808 <https://doi.org/10.1016/j.dsr2.2008.12.009>, 2009.

809 Takahashi, T., Sweeney, C., Hales, B., Chipman, D. W., Newberger, T., Goddard, J. G., Iannuzzi, R. A. and
810 Sutherland, S. C.: The Changing Carbon Cycle in the Southern Ocean, *Oceanography*, 25(3), 26-37,
811 doi:[10/f4bpqs](https://doi.org/10.1016/j.dsr2.2008.12.009), 2012.

812 Tamura, T., Ohshima, K. I., Fraser, A. D., and Williams, G. D.: Sea ice production variability in Antarctic coastal
813 polynyas, *Journal of Geophysical Research: Oceans*, 121, 2967-2979, <https://doi.org/10.1002/2015JC011537>,
814 2016.

815 Touratier, F., and Goyet, C.: Definition, properties, and Atlantic Ocean distribution of the new tracer TrOCA,
816 *Journal of Marine Systems*, 46, 169-179, <https://doi.org/10.1016/j.jmarsys.2003.11.016>, 2004a.

817 Touratier, F., and Goyet, C.: Applying the new TrOCA approach to assess the distribution of anthropogenic CO₂
818 in the Atlantic Ocean, *Journal of Marine Systems*, 46, 181-197, <https://doi.org/10.1016/j.jmarsys.2003.11.020>,
819 2004b.

820 Touratier, F., Azouzi, L., and Goyet, C.: CFC-11, $\Delta 14\text{C}$ and 3H tracers as a means to assess anthropogenic CO₂
821 concentrations in the ocean, *Tellus B*, 59, 318-325, <https://doi.org/10.1111/j.1600-0889.2006.00247.x>, 2007.

822 Tréguer, P., and Le Corre, P.: Manuel d'analyse des sels nutritifs dans l'eau de mer (utilisation de l'autoanalyseur
823 II Technicon), 2nd ed., 110 pp., L.O.C.U.B.O., Brest, 1975.

824 van Heuven, S. M. A. C., Hoppema, M., Huhn, O., Slagter, H. A., and de Baar, H. J. W.: Direct observation of
825 increasing CO₂ in the Weddell Gyre along the Prime Meridian during 1973–2008, *Deep Sea Research Part II:*
826 *Topical Studies in Oceanography*, 58, 2613-2635, <https://doi.org/10.1016/j.dsr2.2011.08.007>, 2011.

827 van Heuven, S. M. A. C.: Determination of the rate of oceanic storage of anthropogenic CO₂ from measurements
828 in the ocean interior: The South Atlantic Ocean, Doctor of Philosophy, Groningen, 2013.

829 van Heuven, S. M. A. C., Hoppema, M., Jones, E. M., and de Baar, H. J. W.: Rapid invasion of anthropogenic
830 CO₂ into the deep circulation of the Weddell Gyre, *Philosophical Transactions of the Royal Society A:*
831 *Mathematical, Physical and Engineering Sciences*, 372, 20130056, <https://doi.org/10.1098/rsta.2013.0056>, 2014.

832 van Wijk, E. M., and Rintoul, S. R.: Freshening drives contraction of Antarctic Bottom Water in the Australian
833 Antarctic Basin, *Geophysical Research Letters*, 41, 1657-1664, <https://doi.org/10.1002/2013GL058921>, 2014.

834 Vázquez-Rodríguez, M., Touratier, F., Lo Monaco, C., Waugh, D. W., Padin, X. A., Bellerby, R. G. J., Goyet, C.,
835 Metzl, N., Ríos, A. F., and Pérez, F. F.: Anthropogenic carbon distributions in the Atlantic Ocean: data-based
836 estimates from the Arctic to the Antarctic, *Biogeosciences*, 6, 439-451, <https://doi.org/10.5194/bg-6-439-2009>,
837 2009.

838 Vernet, M., Geibert, W., Hoppema, M., Brown, P. J., Haas, C., Hellmer, H. H., Jokat, W., Jullion, L., Mazloff, M.,
839 Bakker, D. C. E., Brearley, J. A., Croot, P., Hattermann, T., Hauck, J., Hillenbrand, C. D., Hoppe, C. J. M., Huhn,
840 O., Koch, B. P., Lechtenfeld, O. J., Meredith, M. P., Naveira Garabato, A. C., Nöthig, E. M., Peeken, I., Rutgers
841 van der Loeff, M. M., Schmidtke, S., Schröder, M., Strass, V. H., Torres-Valdés, S., and Verdy, A.: The Weddell
842 Gyre, Southern Ocean: Present Knowledge and Future Challenges, *Reviews of Geophysics*, 57, 623-708,
843 <https://doi.org/10.1029/2018RG000604>, 2019.

844 Waugh, D. W., Hall, T. M., McNeil, B. I., Key, R., and Matear, R. J.: Anthropogenic CO₂ in the oceans estimated
845 using transit time distributions, *Tellus B: Chemical and Physical Meteorology*, 58, 376-389,
846 <https://doi.org/10.1111/j.1600-0889.2006.00222.x>, 2006.

847 Weiss, R. F.: The solubility of nitrogen, oxygen and argon in water and seawater, *Deep Sea Research and*
848 *Oceanographic Abstracts*, 17, 721-735, [https://doi.org/10.1016/0011-7471\(70\)90037-9](https://doi.org/10.1016/0011-7471(70)90037-9), 1970.

849 Williams, G. D., Bindoff, N. L., Marsland, S. J., and Rintoul, S. R.: Formation and export of dense shelf water
850 from the Adélie Depression, East Antarctica, *Journal of Geophysical Research: Oceans*, 113, C04039,
851 <https://doi.org/10.1029/2007JC004346>, 2008.

852 Williams, G. D., Aoki, S., Jacobs, S. S., Rintoul, S. R., Tamura, T., and Bindoff, N. L.: Antarctic Bottom Water
853 from the Adélie and George V Land coast, East Antarctica (140–149°E), *Journal of Geophysical Research: Oceans*,
854 115, C04027, <https://doi.org/10.1029/2009JC005812>, 2010.

855 Williams, G. D., Herraiz-Borreguero, L., Roquet, F., Tamura, T., Ohshima, K. I., Fukamachi, Y., Fraser, A. D.,
856 Gao, L., Chen, H., McMahon, C. R., Harcourt, R., and Hindell, M.: The suppression of Antarctic bottom water
857 formation by melting ice shelves in Prydz Bay, *Nature Communications*, 7, 12577,
858 <https://doi.org/10.1038/ncomms12577>, 2016.

859 Williams, N. L., Feely, R. A., Sabine, C. L., Dickson, A. G., Swift, J. H., Talley, L. D., and Russell, J. L.:
860 Quantifying anthropogenic carbon inventory changes in the Pacific sector of the Southern Ocean, *Marine*
861 *Chemistry*, 174, 147-160, <https://doi.org/10.1016/j.marchem.2015.06.015>, 2015.

862 Williams, N. L., Juranek, L. W., Feely, R. A., Russell, J. L., Johnson, K. S., and Hales, B.: Assessment of the
863 Carbonate Chemistry Seasonal Cycles in the Southern Ocean From Persistent Observational Platforms, *Journal of*
864 *Geophysical Research: Oceans*, 123, 4833-4852, <https://doi.org/10.1029/2017JC012917>, 2018.

865 Yabuki, T., Suga, T., Hanawa, K., Matsuoka, K., Kiwada, H., and Watanabe, T.: Possible source of the antarctic
866 bottom water in the Prydz Bay Region, *Journal of Oceanography*, 62, 649-655, [https://doi.org/10.1007/s10872-](https://doi.org/10.1007/s10872-006-0083-1)
867 [006-0083-1](https://doi.org/10.1007/s10872-006-0083-1), 2006.

868 Yamamoto, A., Abe-Ouchi, A., Shigemitsu, M., Oka, A., Takahashi, K., Ohgaito, R., and Yamanaka, Y.: Global
869 deep ocean oxygenation by enhanced ventilation in the Southern Ocean under long-term global warming, *Global*
870 *Biogeochemical Cycles*, 29, 1801-1815, <https://doi.org/10.1002/2015GB005181>, 2015.

871

872

873

874

875

876

877

878

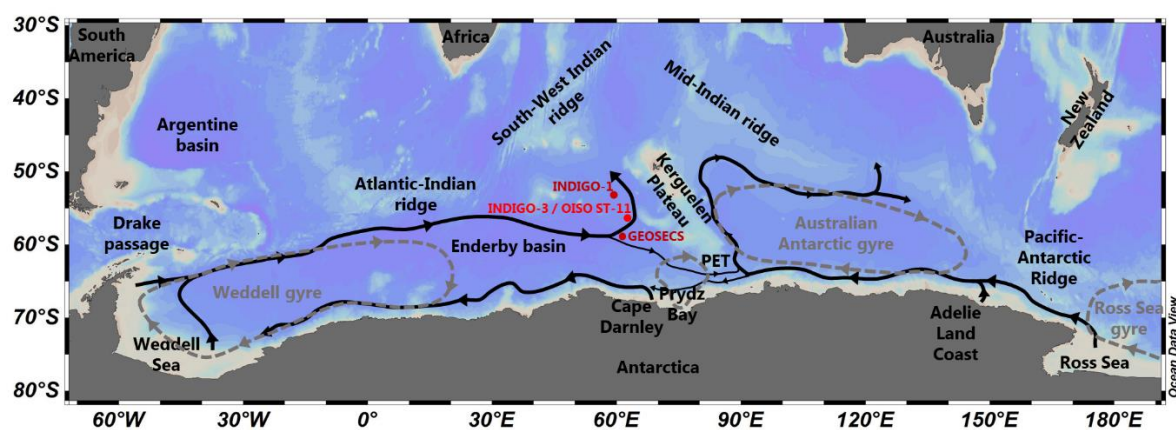
Table 1. List of the cruises used in this study.

Cruise	Station	Location	Year	Month
GEOSECS	430	61.0°E / 60.0°S	1978	February
INDIGO-1	14	58.9°E / 53.0°S	1985	March
INDIGO-3	75	63.2°E / 56.5°S	1987	January
OISO-01	11	63.0°E / 56.5°S	1998	February
OISO-03	11	63.0°E / 56.5°S	1998	December
OISO-05	11	63.0°E / 56.5°S	2000	August
OISO-06	11	63.0°E / 56.5°S	2001	January
OISO-08	11	63.0°E / 56.5°S	2002	January
OISO-11	11	63.0°E / 56.5°S	2004	January
OISO-18	11	63.0°E / 56.5°S	2009	December
OISO-19	11	63.0°E / 56.5°S	2011	January
OISO-21	11	63.0°E / 56.5°S	2012	February
OISO-23	11	63.0°E / 56.5°S	2014	January
OISO-26	11	63.0°E / 56.5°S	2016	October
OISO-27	11	63.0°E / 56.5°S	2017	January
OISO-28	11	63.0°E / 56.5°S	2018	January

880

881

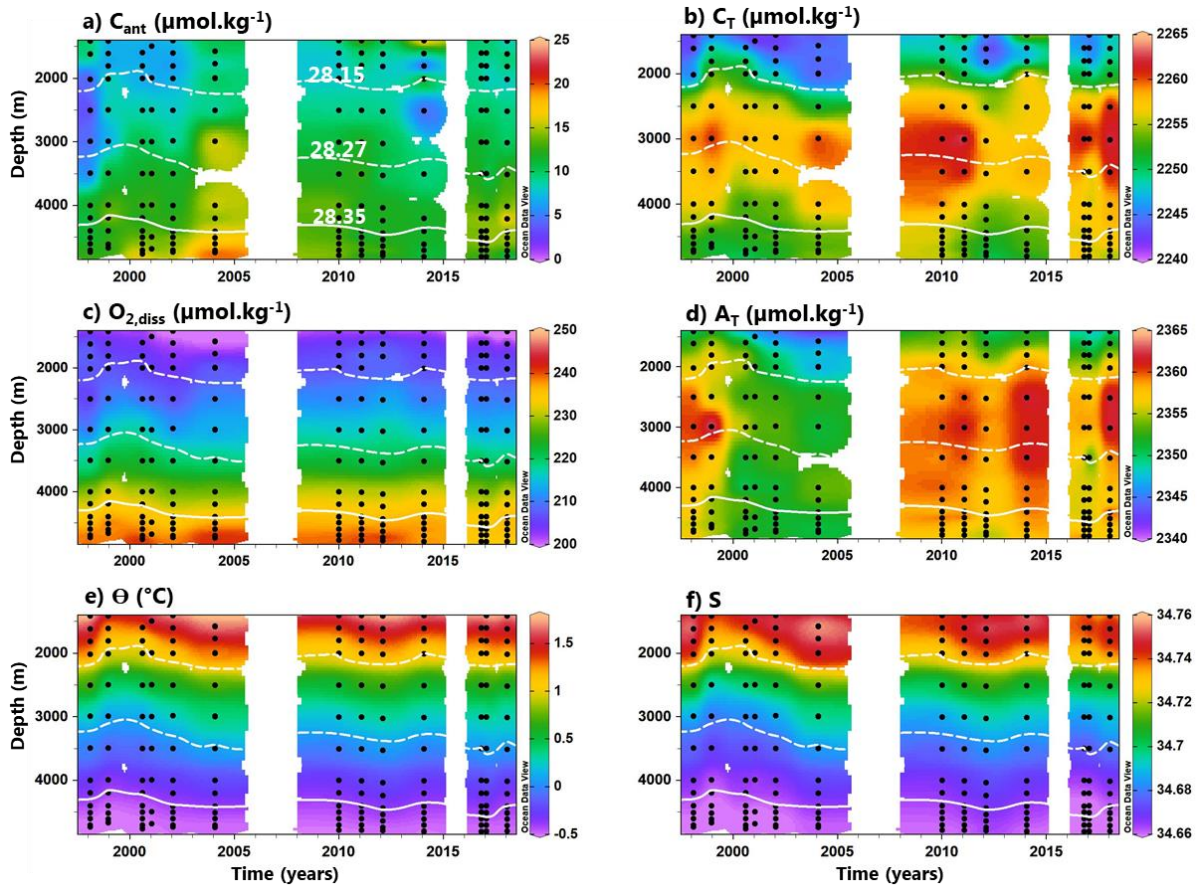
882



883

884 Figure 1. The AABW circulation rough transport paths from the literature (Orsi et al., 1999; Carter et al., 2008;
 885 Fukamachi et al., 2010; Williams et al., 2010; Vernet et al., 2019), with geographic indications (black text), main SO
 886 gyres (dark yellow text and dash lines for the approximative locations) and stations considered in this study (red text
 887 and dots). PET: Princess Elizabeth Trough. Figure produced with ODV (Schlitzer et al., 2019).

888



889

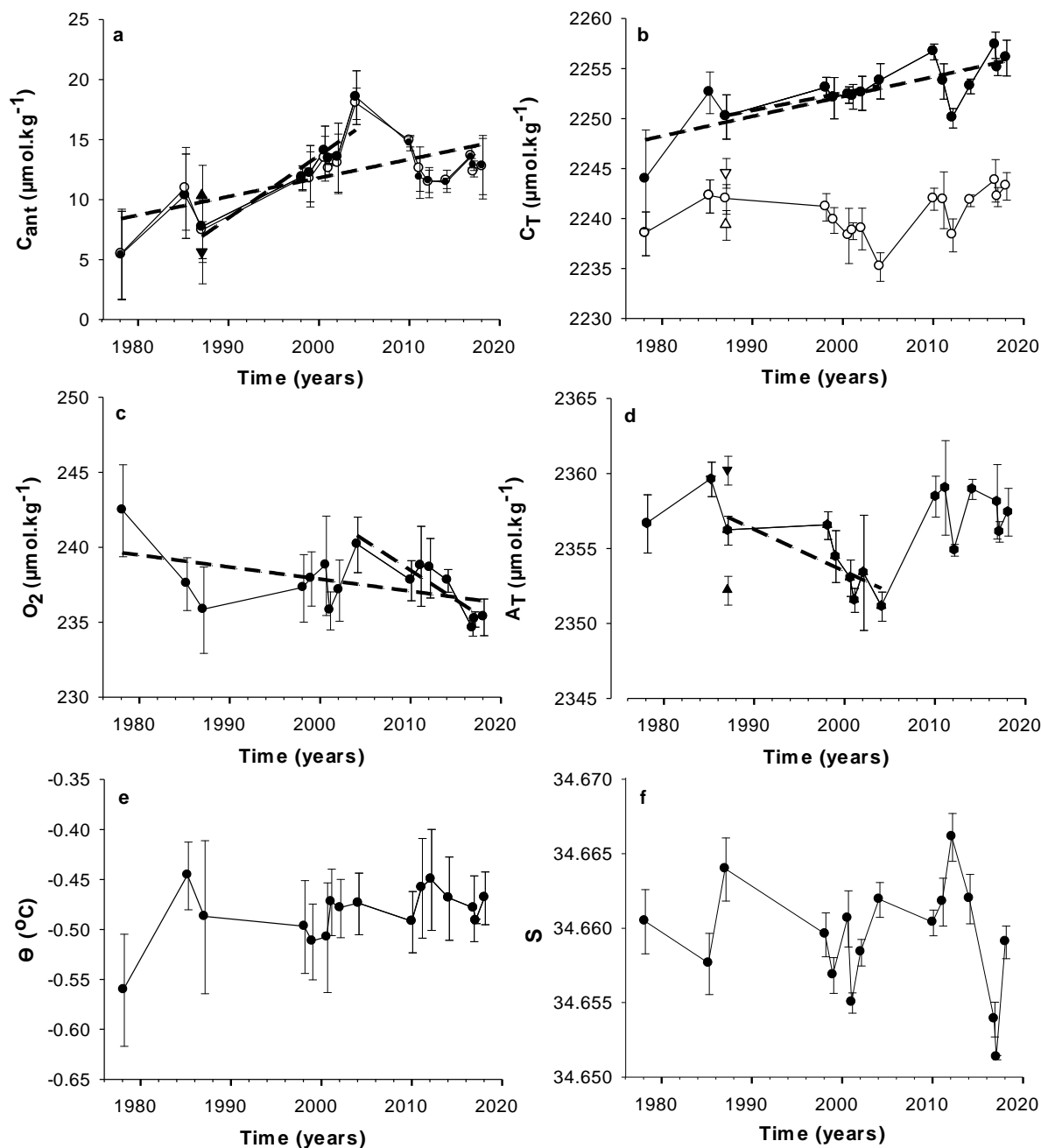
890

891

892

893

Figure 2. Hovmöller diagram of (a) C_{ant} via TrOCA, (b) C_T , (c) O_2 , (d) A_T , (e) θ and (f) S based on the OISO data presented in Table 1. Data points are represented by black dots. The white isolines represent the water masses separation by γ^n (from the bottom: LAABW, UAABW and LCDW). Figure produced with ODV (Schlitzer et al., 2019).



894
 895 **Figure 3. Interannual variability (dash lines lines) and significant trends (at 95 %, see Table 2; dotted lines) for the 40**
 896 **years of observation of the OISO-ST11 LAABW properties, including (a) C_{ant} by the TrOCA (black circles and**
 897 **triangles) and the C^0 (open circles) method, (b) C_T (black circles) and C_{nat} (open circles), (c) O_2 , (d) A_T , (e) Θ and (f) S .**
 898 **For (a) C_{ant} , (b) C_{nat} and (d) A_T , the triangles pointing down and up correspond to INDIGO-3 value without and with -**
 899 **$8 \mu\text{mol.kg}^{-1}$ of correction on the A_T , respectively (see Supp. Mat. for more details).**

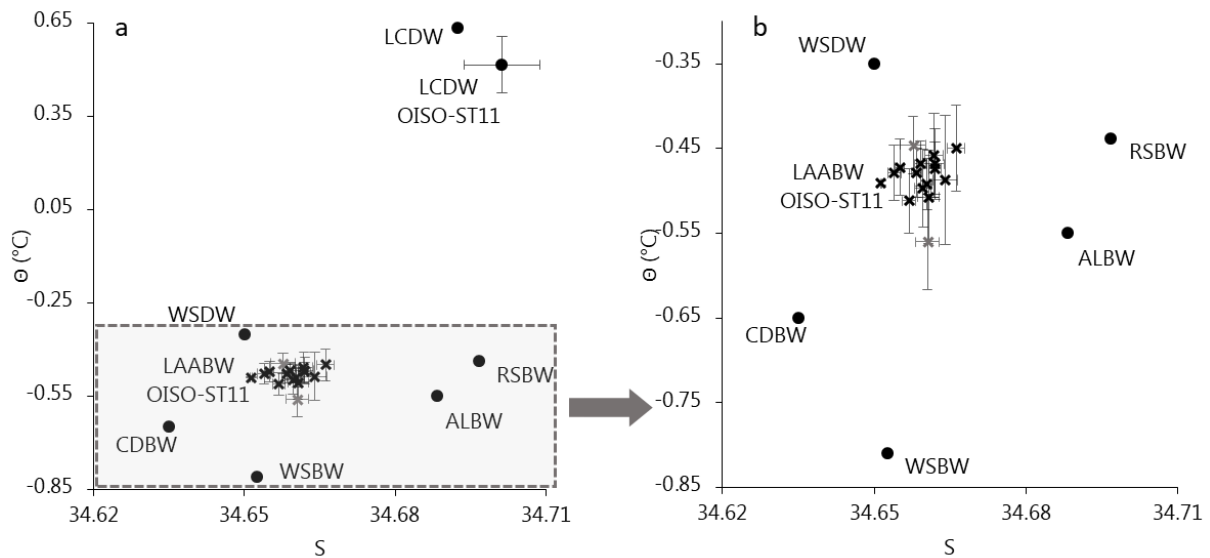
900
 901
 902
 903
 904
 905
 906

907
 908
 909
 910
 911

Table 2: Trends (per decade) of observed and calculated properties in the LAABW estimated over different periods (in bold: significant trends at 95 % confidence level).

Period	S	Θ °C	Si $\mu\text{mol.kg}^{-1}$	NO_3 $\mu\text{mol.kg}^{-1}$	O_2 $\mu\text{mol.kg}^{-1}$	A_T $\mu\text{mol.kg}^{-1}$	C_T $\mu\text{mol.kg}^{-1}$	$\text{C}_{\text{ant TrOCA}}$ $\mu\text{mol.kg}^{-1}$
1978-2018	-0.001 \pm 0.001	0.01 \pm 0.01	-1.2 \pm 0.9	0.2 \pm 0.2	-0.8 \pm 0.4	-0.1 \pm 0.1	2.0 \pm 0.5	1.4 \pm 0.5
1987-2018	-0.001 \pm 0.001	0.01 \pm 0.01	-1.9 \pm 1.4	0.3 \pm 0.4	-0.3 \pm 0.5	0.6 \pm 0.1	1.6 \pm 0.5	1.1 \pm 0.8
1987-2004	-0.003 \pm 0.002	0.01 \pm 0.01	-6.5 \pm 1.8	0.9 \pm 0.9	1.7 \pm 1.0	-1.9 \pm 1.1	1.8 \pm 0.4	5.2 \pm 1.1
2004-2018	-0.006 \pm 0.003	0.01 \pm 0.01	-1.8 \pm 4.5	-0.5 \pm 1.0	-3.9 \pm 0.7	3.4 \pm 0.2	1.7 \pm 1.9	-3.5 \pm 1.5

912



913
 914
 915
 916
 917
 918
 919
 920
 921
 922
 923

Figure 4. (a) Full Θ -S diagram of studied water masses and (b) zoomed on bottom waters. Values are from literature for the WSBW (Fukamachi et al., 2010; van Heuven, 2013; Pardo et al., 2014; Robertson et al., 2002), the WSDW (Carmack and Foster, 1975; Fahrback et al., 1994; van Heuven, 2013; Robertson et al., 2002), the RSBW (Fukamachi et al., 2010; Gordon et al., 2015; Johnson, 2008; Pardo et al., 2014), the ALBW (Fukamachi et al., 2010; Johnson, 2008; Pardo et al., 2014), the CDBW (Ohshima et al., 2013) and the LCDW (Lo Monaco et al., 2005a; Pardo et al., 2014; Smith and Treguer, 1994), and from the OISO-ST11 dataset for the OISO-ST11 LAABW and OISO-ST11 LCDW. Error bars are calculated from the individual annual averaged values for the OISO-ST11 LAABW and from all data for the OISO-ST11 LCDW. For the OISO-ST11 LAABW, the grey cross are the GEOSECS (lowest Θ) and INDIGO-1 (highest Θ) values.

924 **Table 3. Compilation of C_{ant} sequestration investigations in the AABW ($\gamma^n \geq 28.25 \text{ kg.m}^{-3}$) using the TrOCA method.**
 925 **The C_{ant} estimation of Pardo et al. (2014) is calculated using theoretical AABW mean composition (with 3% of ALBW)**
 926 **and the carbon data from the GLODAPv1 and CARINA databases. Sandrini et al. (2007) values has been measured at**
 927 **the bottom in the Ross Sea and correspond to recently sink high salinity shelf water (HSSW). The mean values published**
 928 **by Roden et al. (2016) for the AABW present WSDW characteristics but can be a mix of CDBW and LCDW.**

Source	Location	Water masses considered	Year	C_{ant} $\mu\text{mol.kg}^{-1}$
Pardo et al. (2014) Fig. 5	Averaged AABW composition	WSBW-RSBW-ALBW	1994	12
Lo Monaco et al. (2005b) Fig. 4b	WOCE line I6 (30° E; 50°-70° S)	WSBW CDBW	1996	15 20
Sandrini et al. (2007) Fig. 4a	Ross Sea	HSSW (previous RSBW)	2002/2003	Max. of 30
Shadwick et al. (2014) Table 2	Mertz polynya and Adelie depression	ALBW	2007/2008	15
Roden et al. (2016) Table 2	South Indian ocean (30°-80° E; 60°-69° S)	WSDW-LCDW- CDBW	2006	25
van Heuven et al. (2011) Fig.13	Weddell gyre (0° E; 55°-71°S)	WSBW	2005	16
			1978-1987	8 ± 3
			1987-1998	10 ± 4
		LAABW (mix of WSDW- CDBW-RSBW- ALBW)	1987-2004	13 ± 4
			1998-2004	14 ± 2
			2010-2018	13 ± 1
			1978-2018	12 ± 3

929

930

931